# REPORT DOCUMENTATION PAGE

Form Approved OMB NO. 0704-0188



| 1. REPORT DATE (DD-MM-YYYY) | 2. REPORT TYPE | 3. DATES COVERED (From - To) |
|---|---|---|
| 30-09-2008 | Final Report | 1-Jul-2004 - 30-Jun-2008 |

4. TITLE AND SUBTITLE
Solid State Quantum Computer in Silicon

5a. CONTRACT NUMBER
W911NF-04-1-0290

5b. GRANT NUMBER

5c. PROGRAM ELEMENT NUMBER

6. AUTHORS
Professor R.G. Clark, Professor A.S. Dzurak, Professor M.Y. Simmons, Professor D.N. Jamieson, Professor S. Prawer, Professor L.C.L. Hollenberg, Dr J.C. McCallum

5d. PROJECT NUMBER

5e. TASK NUMBER
611102

5f. WORK UNIT NUMBER
611102

7. PERFORMING ORGANIZATION NAMES AND ADDRESSES
University of New South Wales
Research Office
University of New South Wales
Sydney, AU 2052 -

8. PERFORMING ORGANIZATION REPORT NUMBER

9. SPONSORING/MONITORING AGENCY NAME(S) AND ADDRESS(ES)
U.S. Army Research Office
P.O. Box 12211
Research Triangle Park, NC 27709-2211

10. SPONSOR/MONITOR'S ACRONYM(S)
ARO

11. SPONSOR/MONITOR'S REPORT NUMBER(S)
46422-PH-QC.1

12. DISTRIBUTION AVAILIBILITY STATEMENT
Approved for public release; federal purpose rights

13. SUPPLEMENTARY NOTES
The views, opinions and/or findings contained in this report are those of the author(s) and should not contrued as an official Department of the Army position, policy or decision, unless so designated by other documentation.

14. ABSTRACT
See cover page of Scientific Progress Report - 210631.pdf.

15. SUBJECT TERMS
Quantum Computing

| 16. SECURITY CLASSIFICATION OF: | | | 17. LIMITATION OF ABSTRACT | 15. NUMBER OF PAGES | 19a. NAME OF RESPONSIBLE PERSON |
|---|---|---|---|---|---|
| a. REPORT | b. ABSTRACT | c. THIS PAGE | | | Robert Clark |
| UU | U | U | SAR | | 19b. TELEPHONE NUMBER +61-293-8545 |

**Report Title**

Solid State Quantum Computer in Silicon

**ABSTRACT**

See cover page of Scientific Progress Report - 210631.pdf.

---

**List of papers submitted or published that acknowledge ARO support during this reporting period. List the papers, including journal references, in the following categories:**

**(a) Papers published in peer-reviewed journals (N/A for none)**

S.J. Angus, A.J. Ferguson, A.S. Dzurak and R.G. Clark, “A silicon radio-frequency single electron transistor”, Applied Physics Letters 92, 112103 (2008).

M.C. Cassidy, A.S. Dzurak, R.G. Clark, K.D. Petersson, I. Farrer, D.A. Ritchie and C.G. Smith, “Single shot charge detection using a radio-frequency quantum point contact” Applied Physics Letters 91, 222104 (2007).

J.H. Cole, A.D. Greentree, L.C.L. Hollenberg, “Spatial adiabatic passage in a realistic triple well structure”. Physical Review B77, 235418 (2008).

N.A. Court, A.J. Ferguson and R.G. Clark, “Energy gap measurement of nanostructured aluminium thin films for single Cooper-pair devices”, Superconductor Science and Technology 21, 015013 (2008).

N.A. Court, A.J. Ferguson and R.G. Clark, “A quantitative study of quasiparticle traps using the single-Cooper pair- transistor”, Physics Review B (Rapid Communications) 77, 100501 (2008).

S.J. Devitt, A.D. Greentree, R. Ionicioiu, J.L. O’Brien, W.J. Munro and L.C.L. Hollenberg, “Photonic module: An on-demand resource for photonic entanglement”, Physical Review A 76, 052312 (2007).

S.J. Devitt, A.D. Greentree and L.C.L. Hollenberg, “Information free quantum bus for generating stabilizer states”, Quantum Information Processing 6, 229 (2007).

S.J Devitt, S.G. Schirmer, D.K.L. Oi, J.H. Cole and L.C.L. Hollenberg, “Subspace confinement: how good is your qubit?”, New Journal of Physics 9, 384 (2007).

M. Füchsle, F.J. Ruess, T.C.G. Reusch, M. Mitic and M.Y. Simmons, “Surface gate and contact alignment for buried, atomically precise STM-patterned devices”, Journal of Vacuum Science and Technology B 25, 2562 (2007).

K.E.J. Goh, M.Y. Simmons, and A.R. Hamilton, “Electron-electron interactions in highly disordered two-dimensional systems”, Physical Review B 77, 235410 (2008).

K.E.J. Goh, M.Y. Simmons and A. R. Hamilton, “Use of low-temperature Hall effect to measure dopant activation: Role of electron-electron interactions”, Physical Review B 76, 193305 (2008).

T. Hallam, M.J. Butcher, K.E.J. Goh and M.Y. Simmons, “Use of a SEM to pattern large areas of a hydrogen resist for electrical contacts”, Journal of Applied Physics 102, 034308 (2007).

T. Hopf, C. Yang, S.M. Hearne, D.N. Jamieson, E. Gauja, S.E. Andresen, and A.S. Dzurak, “Low-noise detection system for the counted implantation of single ions in silicon”, IEEE Transactions on Nuclear Science, 55, 812 (2008).

F.E. Hudson, A.J. Ferguson, C.C. Escott, C. Yang, D.N. Jamieson, R.G. Clark and A.S. Dzurak, "Gate-controlled charge transfer in Si:P double quantum dots", Nanotechnology 19, 195402 (2008).

G.P. Lansbergen, R. Rahman, C.J. Wellard, I. Woo, J. Caro, N. Collaert, S. Biesemans, G. Klimeck, L.C.L. Hollenberg and S. Rogge, “Gate-induced quantum confinement transition of a single dopant atom in a Si FinFET”, Nature Physics 4, 656 (2008).

M.I. Makin, J.H. Cole, C. Tahan, L.C.L. Hollenberg and A.D. Greentree, “Quantum phase transitions in photonic cavities with two-level systems”, Physical Review A 77, 053819 (2008).

M. Mitic, K.D. Petersson, M.C. Cassidy, R.P. Starrett, E. Gauja, A.J. Ferguson, C. Yang, D.N. Jamieson, R.G. Clark and A.S. Dzurak, “Bias spectroscopy and simultaneous single-electron transistor charge state detection of Si:P double dots”, Nanotechnology 19, 265201 (2008).

A. Morello and L.J. de Jongh, “Dynamics and thermalization of the nuclear spin bath in the single-molecule magnet Mn12-ac: Test for the theory of spin tunnelling”, Physical Review B 76, 184425 (2007).

M.W. Radny, P.V. Smith, T.C.G. Reusch, O. Warschkow, N.A. Marks, H.F. Wilson, S.R. Schofield, N.J. Curson, D.R. McKenzie and M.Y. Simmons, “Single hydrogen atom on the Si(001) surface”, Physical Review B 76, 155302 (2007).

M.W. Radny, P.V. Smith, T.C.G. Reusch, O. Warschkow, N.A. Marks, H.Q. Shi, D.R. McKenzie, S.R. Schofield, N.J. Curson and M.Y. Simmons, “Single P and As dopants in the Si(001) surface”, Journal of Chemical Physics 127, 184706 (2007).

T.C.G. Reusch, O. Warschkow, M.W. Radny, P.V. Smith, N.A. Marks, N.J. Curson, D.R. McKenzie and M.Y. Simmons, “Doping and STM tip-induced changes to dangling bonds on Si(001)”, Surface Science 601, 4036 (2007).

T.C.G. Reusch, K.E.J. Goh, W. Pok, N.Lo, S. McKibbin and M.Y. Simmons, “Morphology and electrical conduction of Si:P delta-doped layers on vicinal Si(001)" accepted for Journal of Applied Physics (2008).

F. J. Ruess, B. Weber, O. Kocklan, A. R. Hamilton and M. Y. Simmons, “1D conduction properties of highly phosphorus doped planar nanowires patterned by scanning probe microscopy”, Physical Review B 76, 085403 (2007).

F.J. Ruess, W. Pok, T.C.G. Reusch, G. Scappucci, M. Füchsle, M. Mitic, D.L. Thompson and M.Y. Simmons, “Structural integrity and transport characteristics of STM-defined, highly doped Si:P nanodots”, Journal of Scanning Probe Microscopy 2, 10 (2007).

F.J. Ruess, A.P. Micolich, W. Pok, K.E.J. Goh, A.R. Hamilton and M.Y. Simmons, “Ohmic conduction of sub-10 nm P-doped silicon nanowires at cryogenic temperatures”, Applied Physics Letters 92, 052101 (2008).

F.J. Ruess, G. Scappucci, M. Füchsle, W. Pok, A. Fuhrer, D. L. Thompson, T.C.G. Reusch, and M.Y. Simmons, "Demonstration of gating action in atomically controlled Si:P nanodots defined by scanning probe microscopy", Physica E 40, 1006 (2008).

G. Scappucci, F. Ratto, D.L. Thompson, T.C.G. Reusch, W. Pok, F.J. Ruess, F. Rosei and M.Y. Simmons, “Structural and electrical characterization of room temperature ultra-high-vacuum compatible SiO2 for gating scanning tunneling microscope-patterned devices”, Applied Physics Letters 91, 222109 (2007).

D. Schröer, A.D. Greentree, L. Gaudreau, K. Eberl, L.C.L. Hollenberg, J.P. Kotthaus and S. Ludwig, “Electrostatically defined serial triple quantum dot charged with few electrons”, Physical Review B 76, 075306 (2007).

M.Y. Simmons, "Probing dopants at the atomic level”, Nature Physics 4,165 (2008).

M.Y. Simmons, F.J. Ruess, K.E.J. Goh, W. Pok, T. Hallam, M.J. Butcher, T.C.G. Reusch, G. Scappucci, A.R. Hamilton and L. Oberbeck, “Atomic scale device fabrication”, International Journal of Nanotechnology 5, 352 (2008).

M.Y. Simmons, F.J. Ruess, W. Pok, D.L. Thompson, M. Füchsle, G. Scappucci,T.C.G. Reusch, K.E.J. Goh, S.R. Schofield, B. Weber, L. Oberbeck, A.R. Hamilton and F. Ratto, “Atomically Precise Silicon Device Fabrication”, accepted for the IEEE Transactions on Nanotechnology (2007).

A.M. Stephens, Z.W.E. Evans, S.J. Devitt and L.C.L. Hollenberg, “Asymmetric quantum error correction via code conversion”, Physical Review A 77, 062335 (2008).

A.M. Stephens, A.G. Fowler and L.C.L. Hollenberg, “Universal fault tolerant quantum computation on bilinear nearest neighbour arrays”, Quantum Information and Computation 8, 330 (2008).

L.H. Willems van Beveren, H. Huebl, D.R. McCamey, T. Duty, A.J. Ferguson, R.G. Clark and M.S. Brandt, “Broadband electrically detected magnetic resonance of phosphorus donors in a silicon field-effect transistor”, Applied Physics Letters 93, 072102 (2008).

**Number of Papers published in peer-reviewed journals:** 34.00

---

### (b) Papers published in non-peer-reviewed journals or in conference proceedings (N/A for none)

None.

**Number of Papers published in non peer-reviewed journals:** 0.00

---

### (c) Presentations

S.R. Ekanayake, "Quantum Bit Controller and Observer Circuits in SOS-CMOS Technology for Gigahertz Low-Temperature Operation", Contributed Oral Presentation: 7th IEEE International Conference on Nanotechnology, Hong Kong, China, 02–05/08/2007.

F.J. Ruess, "Atomically Controlled Si:P Devices Created by Scanning Probe Microscopy", Contributed Oral presentation: 7th IEEE Conference on Nanotechnology, Hong Kong, China, 02–05/08/2007.

R.G. Clark, "Towards a Solid State Quantum Computer in Silicon",
PI Presentation: US Quantum Computing Program Review Minneapolis, USA, 12–16/08/2007.

O. Warschkow, S.R. Schofield, M.W. Radny, P.V. Smith, N.A. Marks, G. Scappucci, F. Ratto, D.L. Thompson, D.R. McKenzie and M.Y. Simmons,
"Towards an Atomic-Scale Understanding of Silicon Dioxide Gate Dielectric Growth", Poster Presentation: US Quantum Computing Program Review Minneapolis, USA, 12–16/08/2007.

M.Y. Simmons, "Atomic-scale device fabrication in silicon", Invited Talk: TECHCON Conference, Austin, Texas, USA, 8–12/09/2007.

W. Clarke (on behalf of Michelle Simmons), "Scanning probes for silicon device fabrication", Invited Talk: 12th International COMMS Conference, Melbourne, Australia, 04/09/2007.

G.C. Tettamanzi, "Nanoscale Superconducting Electronics",
Contributed Oral Presentation: 8th European Conference on Applied Superconductivity Bruxelles, Belgium, 16–20/09/2007.

M.Y. Simmons, "Atomic-scale device fabrication in silicon", Invited Talk: Nanostructures for Electronics Energy and Environment, Queensland, Australia, 23–28/09/2007.

G. Scappucci, "Low temperature UHV compatible dielectric for gating atomically controlled devices", Invited Talk: Nanostructures for Electronics Energy and Environment, Queensland, Australia, 23–28/09/2007.

D.N. Jamieson, "Ion Beam Physics in Nanotechnology and the Environment", Invited Talk: Nanostructures for Electronics Energy and Environment Queensland, Australia, 23–28/09/2007.

D.N. Jamieson, Single Atom Quantum Devices by Ion Lithography for Information Processing and Transmission", Invited Talk: Nanostructures for Electronics Energy and Environment, Queensland, Australia, 23–28/09/2007.

G. Scappucci, "Low Temperature UHV-Compatible Silicon Dioxide for Gating Atomically Precise Devices in Silicon", Invited Talk: Nanostructures for Electronics Energy and Environment, Queensland, Australia, 23–28/09/2007.

G.C. Tettamanzi, "Nanoscale Superconducting Electronics", Poster Presentation: Nanostructures for Electronics Energy and Environment, Queensland, Australia, 23–28/09/2007.

M.Y. Simmons, "Atomic-scale device fabrication in silicon", Invited Talk: Productive Nanosystems at the Foresight Institute, Arlington, Virginia, USA 9-10/10/2007.

M.Y. Simmons, "Nanoscale device fabrication by scanning probe microscopy", 54th American Vacuum Society Conference, Seattle, USA 14-19/10/2007.

R.G. Clark, "Silicon Quantum Computer: A Decade of Developing the Pieces – A Blueprint for their Assembly", Invited Talk: Military Communications and Information Systems, Canberra, Australia, 20–22/11/2007.

L.H. Willems van Beveren, "Electrically Detected Magnetic Resonance in Accumulation-Layer MOSFETs", Contributed Oral Presentation: 15th AINSE Conference on Nuclear and Complementary Techniques of Analysis & 10th Vacuum Society of Australia Congress, Melbourne, Australia, 21–23/11/2007.

N. Stavrias, "Photoluminescence Investigation of Ion Implanted Phosphorus in Silicon", Poster Presentation: 15th AINSE Conference on Nuclear and Complementary Techniques of Analysis & 10th Vacuum Society of Australia Congress, Melbourne, Australia, 21–23/11/2007.

C.T. Chang, "DLTS Study of Ion and Molecular Implantation Damage in Silicon", Poster Presentation: 15th AINSE Conference on Nuclear and Complementary Techniques of Analysis & 10th Vacuum Society of Australia Congress, Melbourne, Australia, 21–23/11/2007.

D. Pyke, "Raman Measurements of Hydrogen Ions Implanted into Silicon", Poster Presentation: 15th AINSE Conference on Nuclear and Complementary Techniques of Analysis & 10th Vacuum Society of Australia Congress, Melbourne, Australia, 21–23/11/2007.

D. Pyke, "Hydrogen Refinement During Solid Phase Epitazial Crystallisation of Buried Amorphous Silicon Layers", Poster Presentation: 15th AINSE Conference on Nuclear and Complementary Techniques of Analysis & 10th Vacuum Society of Australia Congress, Melbourne, Australia, 21–23/11/2007.

P. Spizzirri, "A TEM Study of Si-SiO2 Interfaces in Silicon Nanodevices", Poster Presentation: 15th AINSE Conference on Nuclear and Complementary Techniques of Analysis & 10th Vacuum Society of Australia Congress, Melbourne, Australia, 21–23/11/2007.

P. Spizzirri, "Characterisation of High Quality, Thermally Grown Silicon Dioxide on Silicon", Poster Presentation: 15th AINSE Conference on Nuclear and Complementary Techniques of Analysis & 10th Vacuum Society of Australia Congress, Melbourne, Australia, 21–23/11/2007.

P. Spizzirri, "An EPR on the Activation of Low Energy Phosphorus Ions Implanted into Silicon", Poster Presentation: 15th AINSE Conference on Nuclear and Complementary Techniques of Analysis & 10th Vacuum Society of Australia Congress, Melbourne, Australia, 21–23/11/2007.

A. Alves, "Detection and Placement of Single Ions in the keV and MeV Regimes: MeV Ion-Aperture Scattering", Poster Presentation: 15th AINSE Conference on Nuclear and Complementary Techniques of Analysis & 10th Vacuum Society of Australia Congress, Melbourne, Australia, 21–23/11/2007.

L.M. Jong, "Identification of Ion Strike Location by Precision IBIC", Poster Presentation: 15th AINSE Conference on Nuclear and Complementary Techniques of Analysis & 10th Vacuum Society of Australia Congress, Melbourne, Australia, 21–23/11/2007.

J.A. van Donkelaar, "Single Ion Implantation using Nano- Apertures: Precision Placement for CTAP", Poster Presentation: 15th AINSE Conference on Nuclear and Complementary Techniques of Analysis & 10th Vacuum Society of Australia Congress, Melbourne, Australia, 21–23/11/2007.

B. Vilis, "A Low Energy, Angle Dependent, Defect Study of H Implanted Si", Poster Presentation: 15th AINSE Conference on Nuclear and Complementary Techniques of Analysis & 10th Vacuum Society of Australia Congress, Melbourne, Australia, 21–23/11/2007.

M. Dunn, "Interface Trap Density Reduction in Thin Silicon Oxides using Ion Implantation", Contributed Oral Presentation: 15th AINSE Conference on Nuclear and Complementary Techniques of Analysis & 10th Vacuum Society of Australia Congress, Melbourne, Australia, 21–23/11/2007.

M.Y. Simmons, "Electron transport through dopants in silicon", Invited Talk: SPIE Microelectronics, MEMS and Nanotechnology, Canberra, Australia 06/12/2007.

R.G. Clark, "Current Status and Future Prospects for QIP in Si:P MOS Architectures Incorporating Single Atom Spintronics", Invited Talk: 2nd Annual Dodd-Walls Symposium, Dunedin, New Zealand, 11-12/02/2008.

M.Y. Simmons, "Silicon Quantum Computing", Invited speaker, International Research Workshop, UNSW, Australia, 21/02/2008

L.C.L. Hollenberg, "Quantum Nanoelectronics to Quantum Information Processing", Invited Talk: International Conference on Nanoscience and Nanotechnology, Melbourne, Australia, 25-29/02/2008.

M. Makin, "Phase Transitions in Photonic Cavities: Exact vs. Mean-Field", Contributed Oral Presentation: International Conference on Nanoscience and Nanotechnology< Melbourne, Australia, 25-29/02/2008.

C. Yang, "Development of Single Ion Implantation Technology",
Oral Presentation: International Conference on Nanoscience and Nanotechnology, Melbourne, Australia, 25-29/02/2008.

B. Villis, "Dislocation Related Band-Edge Photoluminescence in Boron-Implanted Silicon", Oral Presentation: International Conference on Nanoscience and Nanotechnology, Melbourne, Australia, 25-29/02/2008.

D. Drumm, "Ab-Initio Calculations of Xe-Based Optical Centres in Diamond", Oral Presentation: International Conference on Nanoscience and Nanotechnology, Melbourne, Australia, 25-29/02/2008.

A.D. Greentree, "Spatial Adiabatic Passages as a Quantum Wire",
Oral Presentation: International Conference on Nanoscience and Nanotechnology, Melbourne, Australia, 25-29/02/2008.

N. Stavrias, "Photoluminescence of Silicon for the Silicon Quantum Computer", Oral Presentation: International Conference on Nanoscience and Nanotechnology, Melbourne, Australia, 25-29/02/2008.

L.H. Willems van Beveren, H. Huebl, T. Duty, D.R. McCamey, A.J. Ferguson, M.S. Brandt, and R.G. Clark, "Electrically Detected Magnetic Resonance in Accumulation-layer MOSFETs", Contributed Oral Presentation: International Conference on Nanoscience and Nanotechnology, Melbourne, Australia, 25-29/02/2008.

A. Morello, C. Escott, L.H. Willems van Beveren, H. Huebl, L.C.L. Hollenberg, D.N. Jamieson, A.S. Dzurak and R.G. Clark, "Architecture for Coherent Control and Readout of the Electron Spin of a Single Donor in Silicon", Contributed Oral Presentation: International Conference on Nanoscience and Nanotechnology, Melbourne, Australia, 25-29/02/2008.

F.J. Ruess, "Atomically controlled Devices in silicon created by scanning probe microscopy", Contributed speaker, International Conference on Nanoscience & Nanotechnology (ICONN), Melbourne, Australia, 25-29/02/2008.

T.C.G. Reusch, "Nanoscale dopant rings fabricated by STM lithography", Contributed speaker, International Conference on Nanoscience & Nanotechnology (ICONN), Melbourne, Australia, 25-29/02/2008.

S.J. Angus, A.J. Ferguson, A.S. Dzurak and R.G. Clark, "Quantum Dots and rf-SETs in Silicon", Contributed Oral Presentation: International Conference on Nanoscience and Nanotechnology, Melbourne, Australia, 25-29/02/2008.

N. Court, A. Ferguson and R.G. Clark, "A Study of Quasiparticle Traps with the Single Cooper-pair Transistor", Contributed Oral Presentation: International Conference on Nanoscience and Nanotechnology, Melbourne, Australia, 25-29/02/2008.

L.M. Jong, "Coherent Tunnelling Adiabatic Passage with the Alternating Coupling Scheme", Poster Presentation: International Conference on Nanoscience and Nanotechnology, Melbourne, Australia, 25-29/02/2008.

A. Alves, "Nanoscale Ion Beam Induced Charge Mapping Using MeV Ions", Poster Presentation: International Conference on Nanoscience and Nanotechnology, Melbourne, Australia, 25-29/02/2008.

B.C. Johnson, "Dopant Enhanced Hydrogen Diffusion in Amorphouse Silicon Layers Formed by Ion Implantation", Poster Presentation: International Conference on Nanoscience and Nanotechnology, Melbourne, Australia, 25-29/02/2008.

J. van Donkelaar, "Implantation for Triple-Donar CTAP Devices in Silicon", Poster Presentation: International Conference on Nanoscience and Nanotechnology, Melbourne, Australia, 25-29/02/2008.

B. Villis, "Angle Dependent Defect Study of Ion Implanted Si",
Poster Presentation: International Conference on Nanoscience and Nanotechnology, Melbourne, Australia, 25-29/02/2008.

M.Y. Simmons, "Engineered materials for single atom architectures for computation", Invited speaker, 52nd International Conference on Electron, Ion and Photon Beam Nanotechnology (EIPBN), Oregon, USA, 27-30/05/2008.

M.Y. Simmons, "Atomic-Scale Device Fabrication in Silicon",
Invited speaker, 15th International Conference on Molecular Beam Epitaxy (MBE), Taipei, Taiwan, 06-07/06/2008.

M.Y. Simmons, "Atomic Electronic: Precompetitive Research for the Global Semiconductor Industry", Invited speaker, ARC Graeme Clark Research Outcomes Forum, Parliamanet House, Canberra, ACT, 18/06/2008.

A.S. Dzurak, "Silicon-based Qubits and QCA Devices", Invited Talk: Workshop on Low Temperature Electronics 2008, Jena, Germany, 22-24/06/2008.

A.S. Dzurak, "Ion-implanted donor-based qubits in silicon: Single Atom Nanoelectronics", Invited Talk: Spin and Qubit 2008, Copenhagen, Denmark, 02-04/06/2008.

**Number of Presentations:** 55.00

---

## Non Peer-Reviewed Conference Proceeding publications (other than abstracts):

A. Alves, J. van Donkelaar, C. Yang, D.N. Jamieson, M. Taylor and P.N. Johnston, “Detection and placement of single ions in the keV and MeV regimes: MeV ion-aperture scattering”, Proceedings of the 15th Australian Conference on Nuclear and Complimentary Techniques of Analysis and 9th Vacuum Society of Australia Congress, pp 127–132.

C.T. Chang and J.C. McCallum, “DLTS study of ion and molecular implantation damage in silicon”, Proceedings of the 15th Australian Conference on Nuclear and Complimentary Techniques of Analysis and 9th Vacuum Society of Australia Congress, pp 157–160.

M. Dunn, J. McCallum and E. Gauja, “Interface trap density reduction in thin silicon oxides using ion implantation”, Proceedings of the 15th Australian Conference on Nuclear and Complimentary Techniques of Analysis and 9th Vacuum Society of Australia Congress, pp 73–76.

J-H. Fang, P. Spizzirri, A. Cimmino and S. Prawer, “Fabrication of periodic Al2O3 nanomasks”, Proceedings of the 15th Australian Conference on Nuclear and Complimentary Techniques of Analysis and 9th Vacuum Society of Australia Congress, pp 179–181.

V.S. Gill, D.X. Belton, D.N. Jamieson and C.G Ryan, “Age mapping of radioisotopes by daughter trace elements analysis”, Proceedings of the 15th Australian Conference on Nuclear and Complimentary Techniques of Analysis and 9th Vacuum Society of Australia Congress, pp 185–188.

B.C. Johnson, P. Caradonna and J.C. McCallum, “Dopant enhanced hydrogen diffusion in amorphous silicon layers”, Proceedings of the 15th Australian Conference on Nuclear and Complimentary Techniques of Analysis and 9th Vacuum Society of Australia Congress, pp 202–205.

L.M. Jong, C. Yang, T. Hopf, D.N. Jamieson, E. Gauja, A.S. Dzurak and R.G. Clark, “Identification of ion strike location by precision IBIC”, Proceedings of the 15th Australian Conference on Nuclear and Complimentary Techniques of Analysis and 9th Vacuum Society of Australia Congress, pp 207–210.

D.J. Pyke and J.C. McCallum, “Raman measurements of hydrogen ions implanted into silicon”, Proceedings of the 15th Australian Conference on Nuclear and Complimentary Techniques of Analysis and 9th Vacuum Society of Australia Congress, pp 272–275.

D.J. Pyke and J.C. McCallum, “Hydrogen refinement during solid phase epitazial crystallisation of buried amorphous silicon layers”, Proceedings of the 15th Australian Conference on Nuclear and Complimentary Techniques of Analysis and 9th Vacuum Society of Australia Congress, pp 276–281.

P. Spizzirri, S. Rubanov, E. Gauja, L. Willems van Beveren, R. Brenner and S. Prawer, “A TEM study of Si-SiO2 interfaces in silicon nanodevices”, Proceedings of the 15th Australian Conference on Nuclear and Complimentary Techniques of Analysis and 9th Vacuum Society of Australia Congress, pp 297–300.

P. Spizzirri, J.C. McCallum, M. Dunn, E. Gauja and S. Prawer, “Characterisation of high quality, thermally grown silicon dioxide on silicon”, Proceedings of the 15th Australian Conference on Nuclear and Complimentary Techniques of Analysis and 9th Vacuum Society of Australia Congress, pp 301–304.

P. Spizzirri, J.C. McCallum, W.D. Hutchison, N. Suwuntanasarn, N. Bulatovic, N. Stavrias and S. Prawer, “An EPR study of on the activation of low energy phosphorus ions implanted into silicon”, Proceedings of the 15th Australian Conference on Nuclear and Complimentary Techniques of Analysis and 9th Vacuum Society of Australia Congress, pp 305–309.

J.A. van Donkelaar, A.D. Greentree, A. Alves, C. Yang, S. Rubanov and D.N. Jamieson, “Single ion implantation using nan-apertures: precision placement for CTAP”, Proceedings of the 15th Australian Conference on Nuclear and Complimentary Techniques of Analysis and 9th Vacuum Society of Australia Congress, pp 322–325.

B.J. Villis and J.C. McCallum, “A low energy, angle dependent, defect study of H implanted Si”, Proceedings of the 15th Australian Conference on Nuclear and Complimentary Techniques of Analysis and 9th Vacuum Society of Australia Congress, pp 334–337.

C. Yang, D.N. Jamieson, T. Hopf, E. Gauja, A.S. Dzurak and R.G. Clark, “Avalanche detector technology for keV single ion detection and implantation for quantum bits construction”, Proceedings of the 15th Australian Conference on Nuclear and Complimentary Techniques of Analysis and 9th Vacuum Society of Australia Congress, pp 108–110.

W. Zhang, J. McCallum, D. Sadedin and M. Reuter, “Reduction of titanium dioxide: comparison of analysis by raman spectroscopy and XRD”, Proceedings of the 15th Australian Conference on Nuclear and Complimentary Techniques of Analysis and 9th Vacuum Society of Australia Congress, pp 358–361.

**Number of Non Peer-Reviewed Conference Proceeding publications (other than abstracts):** 16

## Peer-Reviewed Conference Proceeding publications (other than abstracts):

S.R. Ekanayake, T. Lehmann, A.S. Dzurak and R.G. Clark, “Quantum bit controller and observer circuits in SOS-CMOS technology for gigahertz low-temperature operation”, Proceedings of the 7th IEEE International Conference on Nanotechnology, pp 1283–1287.

M.Y. Simmons, F.J. Ruess, W. Pok, D.L. Thompson, M. Füchsle, G. Scappucci, T.C.G. Reusch, K.E.J. Goh, S.R. Schofield, B. Weber, L. Oberbeck, A.R. Hamilton and F. Ratto, “Atomically precise silicon device fabrication”, Proceedings of the 7th IEEE International Conference on Nanotechnology, pp 903-906.

**Number of Peer-Reviewed Conference Proceeding publications (other than abstracts):** 2

## (d) Manuscripts

S.R. Ekanayake, T. Lehmann, A.S. Dzurak, R.G. Clark and A. Brawley, "Characterisation of SOI RF-CMOS FETs at ultra-low temperatures for the design of integrated circuits for quantum bit control and readout" submitted for IEEE Transactions on Electron Devices.

**Number of Manuscripts:** 1.00

**Number of Inventions:**

## Graduate Students

| NAME | PERCENT SUPPORTED |
|---|---|
| Marc Ahrens | |
| Joo Chew Ang | |
| Susan Angus | |
| Maja Cassidy | |
| Victor Chan | |
| Kok Wai Chan | |
| Nadia Court | |
| Simon Devitt | |
| Daniel Drumm | |
| Ramesh Ekanayake | |
| Chris Escott | |
| Zac Evans | |
| Martin Fuechsle | |
| Virginia Gill | |
| Toby Hopf | |
| Lenneke Jong | |
| Gajendran Kandasamy | |
| Wee Han Lim | |
| Graeme Lowe | |
| Melissa Makin | |
| Mladen Mitic | |
| Dane McCamey | |
| Shannon Orbons | |
| Daniel Pyke | |
| Nikolas Stavrias | |
| Ashley Stephens | |
| Chun Hsu Su | |
| Kuan Yen Tan | |
| Matthew Testolin | |
| Giuseppe Tettamanzi | |
| Daniel Thompson | |
| Jessica van Donkelaar | |
| Byron Villis | |
| David Wang | |
| **FTE Equivalent:** | |
| **Total Number:** | **34** |

## Names of Post Doctorates

| NAME | PERCENT SUPPORTED |
|---|---|
| Susan Angus | 0.30 |
| Hans Huebl | 0.00 |
| Fay Hudson | 0.50 |
| Linda Macks | 0.50 |
| Andrea Morello | 1.00 |
| Thilo Reusch | 1.00 |
| Frank Ruess | 0.00 |
| Giordano Scappucci | 0.00 |
| Laurens Willems van Beveren | 0.60 |
| **FTE Equivalent:** | **3.90** |
| **Total Number:** | **9** |

## Names of Faculty Supported

| NAME | PERCENT SUPPORTED | National Academy Member |
|---|---|---|
| Robert Clark | 0.00 | Yes |
| Andrew Dzurak | 0.00 | No |
| Michelle Simmons | 0.00 | Yes |
| David Jamieson | 0.00 | No |
| Steven Prawer | 0.00 | No |
| Lloyd Hollenberg | 0.00 | No |
| Jeff McCallum | 0.00 | No |
| **FTE Equivalent:** | **0.00** | |
| **Total Number:** | **7** | |

## Names of Under Graduate students supported

| NAME | PERCENT SUPPORTED |
|---|---|
| None supported under this QCCM awa | |
| **FTE Equivalent:** | |
| **Total Number:** | **1** |

## Student Metrics

This section only applies to graduating undergraduates supported by this agreement in this reporting period

| | |
|---|---|
| The number of undergraduates funded by this agreement who graduated during this period: ..... | 0.00 |
| The number of undergraduates funded by this agreement who graduated during this period with a degree in science, mathematics, engineering, or technology fields:..... | 0.00 |
| The number of undergraduates funded by your agreement who graduated during this period and will continue to pursue a graduate or Ph.D. degree in science, mathematics, engineering, or technology fields:..... | 0.00 |
| Number of graduating undergraduates who achieved a 3.5 GPA to 4.0 (4.0 max scale): ..... | 0.00 |
| Number of graduating undergraduates funded by a DoD funded Center of Excellence grant for Education, Research and Engineering: ..... | 0.00 |
| The number of undergraduates funded by your agreement who graduated during this period and intend to work for the Department of Defense ..... | 0.00 |
| The number of undergraduates funded by your agreement who graduated during this period and will receive scholarships or fellowships for further studies in science, mathematics, engineering or technology fields: ..... | 0.00 |

## Names of Personnel receiving masters degrees

| NAME |
|---|
| None supported under this QCCM award. |
| **Total Number:** **1** |

## Names of personnel receiving PHDs

| NAME |
|---|
| Joo Chew Ang |
| Susan Angus |
| Nadia Court |
| Gajendran Kandasamy |
| Dane McCamey |
| Mladen Mitic |
| Shannon Orbons |
| **Total Number:** **7** |

## Names of other research staff

| NAME | PERCENT_SUPPORTED | |
|---|---|---|
| David Barber | 1.00 | No |
| Frank Wright | 1.00 | No |
| Venus Lim | 0.50 | No |
| **FTE Equivalent:** | **2.50** | |
| **Total Number:** | **3** | |

## Sub Contractors (DD882)

1 a. The University of Melbourne

1 b. Swanston Street
Parkville
Melbourne VIC 3010

**Sub Contractor Numbers (c):**
**Patent Clause Number (d-1):**
**Patent Date (d-2):**
**Work Description (e):**
**Sub Contract Award Date (f-1):**
**Sub Contract Est Completion Date(f-2):**

1 a. Purdue University

1 b. School of Electrical and Computer Engir

West Lafayette Indiana 47907

**Sub Contractor Numbers (c):**
**Patent Clause Number (d-1):**
**Patent Date (d-2):**
**Work Description (e):**
**Sub Contract Award Date (f-1):**
**Sub Contract Est Completion Date(f-2):**

1 a. University of Calgary

1 b. Earth Sciences 720
2500 University Drive N.W.
Calgary Alberta T2N 1N4

**Sub Contractor Numbers (c):**
**Patent Clause Number (d-1):**
**Patent Date (d-2):**
**Work Description (e):**
**Sub Contract Award Date (f-1):**
**Sub Contract Est Completion Date(f-2):**

## Inventions (DD882)

5 **Components for optical qubits in the radio frequency basis**

Patent Filed in US? (5d-1) Y

Patent Filed in Foreign Countries? (5d-2) Y

Was the assignment forwarded to the contracting officer? (5e) N

Foreign Countries of application (5g-2): Australia

5a: Elanor Huntington

5f-1a: The University of New South Wales - ADFA

5f-c: Northcott Drive

Canberra AC 2600

5a: Timothy Cameron Ralph

5f-1a: The University of Queensland

5f-c: 7 Cooper Road

St Lucia QL 4072

5 **Control and readout of electron or hole spin**

Patent Filed in US? (5d-1) N

Patent Filed in Foreign Countries? (5d-2) Y

Was the assignment forwarded to the contracting officer? (5e) N

Foreign Countries of application (5g-2): Australia

5a: To be advised

5f-1a: The University of New South Wales

5f-c: CQCT, School of Physics

Sydney NS 2052

5 **Electron devices for single electron and nuclear spin resonance**

Patent Filed in US? (5d-1) Y

Patent Filed in Foreign Countries? (5d-2) Y

Was the assignment forwarded to the contracting officer? (5e) N

Foreign Countries of application (5g-2): Australia; China; Europe; India; Japan

5a: Bruce Kane

5f-1a: The University of New South Wales

5f-c: CQCT, School of Physics

Sydney NS 2052

5 **Error corrected quantum computer**

Patent Filed in US? (5d-1) Y

Patent Filed in Foreign Countries? (5d-2) Y

Was the assignment forwarded to the contracting officer? (5e) N

Foreign Countries of application (5g-2): Australia

5a: Cameron Wellard

5f-1a: The University of Melbourne

5f-c: Corner of Swanston Street and Tin Alley

Melbourne VI 3010

5a: Andrew Greentree

5f-1a: The University of Melbourne

5f-c: Corner of Swanston Street and Tin Alley

Melbourne VI 3010

5a: Austin Fowler

5f-1a: The University of Melbourne

5f-c: Corner of Swanston Street and Tin Alley

Melbourne VI 3010

5a: Lloyd Christopher Leonard Hollenberg

5f-1a: The University of Melbourne

5f-c: Corner of Swanston Street and Tin Alley

Melbourne VI 3010

5a: Ashley Stephens

5f-1a: The University of Melbourne

5f-c: Corner of Swanston Street and Tin Alley

Melbourne VI 3010

5 **Fabricating nanoscale and atomic scale devices**

Patent Filed in US? (5d-1) Y

Patent Filed in Foreign Countries? (5d-2) Y

Was the assignment forwarded to the contracting officer? (5e) N

Foreign Countries of application (5g-2): Australia; China; Europe; India; Japan

5a: Frank J. Ruess

5f-1a: The University of New South Wales

5f-c: CQCT, School of Physics

Sydney NS 2052

5a: Lars Oberbeck

5f-1a: The University of New South Wales

5f-c: CQCT, School of Physics

Sydney NS 2052

5a: Toby Hallam

5f-1a: The University of New South Wales

5f-c: CQCT, School of Physics

Sydney NS 2052

5a: Neil Jonathan Curson

5f-1a: The University of New South Wales

5f-c: CQCT, School of Physics

Sydney NS 2052

5a: Rolf Brenner

5f-1a: The University of New South Wales

5f-c: CQCT, School of Physics

Sydney NS 2052

5a: Mladen Mitic

5f-1a: The University of New South Wales

5f-c: CQCT, School of Physics

Sydney NS 2052

5a: Alexander Rudolf Hamilton

5f-1a: The University of New South Wales

5f-c: CQCT, School of Physics

Sydney NS 2052

5a: K.E. Johnson Goh

5f-1a: The University of New South Wales

5f-c: CQCT, School of Physics

Sydney NS 2052

5a: Michelle Yvonne Simmons

5f-1a: The University of New South Wales

5f-c: CQCT, School of Physics

Sydney NS 2052

5 **Fabrication of atomic scale devices**

Patent Filed in US? (5d-1) N

Patent Filed in Foreign Countries? (5d-2) Y

Was the assignment forwarded to the contracting officer? (5e) N

Foreign Countries of application (5g-2): Australia

5a: To be advised

5f-1a: The University of New South Wales

5f-c: CQCT, School of Physics

Sydney NS 2052

5 **Fabrication of nanoelectronic circuits**

Patent Filed in US? (5d-1) Y

Patent Filed in Foreign Countries? (5d-2) Y

Was the assignment forwarded to the contracting officer? (5e) N

Foreign Countries of application (5g-2): Australia

5a: Rita Patricia McKinnon

5f-1a: The University of New South Wales

5f-c: CQCT, School of Physics

Sydney NS 2052

5a: Nancy Ellen Lumpkin

5f-1a: The University of New South Wales

5f-c: CQCT, School of Physics

Sydney NS 2052

5a: Alexander Rudolf Hamilton

5f-1a: The University of New South Wales

5f-c: CQCT, School of Physics

Sydney NS 2052

5a: Andrew Steven Dzurak

5f-1a: The University of New South Wales

5f-c: CQCT, School of Physics

Sydney NS 2052

5a: Robert Graham Clark

5f-1a: The University of New South Wales

5f-c: CQCT, School of Physics

Sydney NS 2052

5a: Tilo Marcus Buehler

5f-1a: The University of New South Wales

5f-c: CQCT, School of Physics

Sydney NS 2052

5a: Rolf Brenner

5f-1a: The University of New South Wales

5f-c: CQCT, School of Physics

Sydney NS 2052

5 **Implanted counted dopant ions**

Patent Filed in US? (5d-1) Y

Patent Filed in Foreign Countries? (5d-2) Y

Was the assignment forwarded to the contracting officer? (5e) N

Foreign Countries of application (5g-2): Australia; China; Europe; India; Japan

5a: Soren Andresen

5f-1a: The University of New South Wales

5f-c: CQCT, School of Physics

Sydney NS 2052

5a: Andrew Steven Dzurak

5f-1a: The University of New South Wales

5f-c: CQCT, School of Physics

Sydney NS 2052

5a: Eric Gauja

5f-1a: The University of New South Wales

5f-c: CQCT, School of Physics

Sydney NS 2052

5a: Sean Hearne

5f-1a: The University of Melbourne

5f-c: Corner of Swanston Street and Tin Alley

Melbourne VI 3010

5a: Toby Felix Hopf

5f-1a: The University of Melbourne

5f-c: Corner of Swanston Street and Tin Alley

Melbourne VI 3010

5a: David Norman Jamieson

5f-1a: The University of Melbourne

5f-c: Corner of Swanston Street and Tin Alley

Melbourne VI 3010

5a: Mladen Mitic

5f-1a: The University of New South Wales

5f-c: CQCT, School of Physics

Sydney NS 2052

5a: Changyi Yang

5f-1a: The University of Melbourne

5f-c: Corner of Swanston Street and Tin Alley

Melbourne VI 3010

5a: Steven Prawer

5f-1a: The University of Melbourne

5f-c: Corner of Swanston Street and Tin Alley

Melbourne VI 3010

5 **Interfacing at low temperature using CMOS technology**

Patent Filed in US? (5d-1) Y

Patent Filed in Foreign Countries? (5d-2) Y

Was the assignment forwarded to the contracting officer? (5e) N

Foreign Countries of application (5g-2): Australia

5a: Andrew Steven Dzurak

5f-1a: The University of New South Wales

5f-c: CQCT, School of Physics

Sydney NS 2052

5a: Sobhath Ramesh Ekanayake

5f-1a: The University of New South Wales

5f-c: CQCT, School of Physics

Sydney NS 2052

5a: Robert Graham Clark

5f-1a: The University of New South Wales

5f-c: CQCT, School of Physics

Sydney NS 2052

5a: Torsten Lehmann

5f-1a: The University of New South Wales

5f-c: CQCT, School of Physics

Sydney NS 2052

5 **Method and system for single ion implantation**

Patent Filed in US? (5d-1) Y

Patent Filed in Foreign Countries? (5d-2) Y

Was the assignment forwarded to the contracting officer? (5e) N

Foreign Countries of application (5g-2): Australia; China; Europe; India; Japan

5a: David Norman Jamieson

5f-1a: The University of Melbourne

5f-c: Corner of Swanston Street and Tin Alley

Melbourne VI 3010

5a: Steven Prawer

5f-1a: The University of Melbourne

5f-c: Corner of Swanston Street and Tin Alley

Melbourne VI 3010

5a: Changyi Yang

5f-1a: The University of Melbourne

5f-c: Corner of Swanston Street and Tin Alley

Melbourne VI 3010

5a: Robert Graham Clark

5f-1a: The University of New South Wales

5f-c: CQCT, School of Physics

Sydney NS 2052

5a: Andrew Steven Dzurak

5f-1a: The University of New South Wales

5f-c: CQCT, School of Physics

Sydney NS 2052

5 **Quantum computer**

Patent Filed in US? (5d-1) Y

Patent Filed in Foreign Countries? (5d-2) Y

Was the assignment forwarded to the contracting officer? (5e) N

Foreign Countries of application (5g-2): Australia, China, Europe, India, Japan

5a: Bruce Kane

5f-1a: The University of New South Wales

5f-c: CQCT, School of Physics

Sydney NS 2052

5 **Qubit readout**

Patent Filed in US? (5d-1) Y

Patent Filed in Foreign Countries? (5d-2) Y

Was the assignment forwarded to the contracting officer? (5e) N

Foreign Countries of application (5g-2): Australia

5a: Lloyd Christopher Leonard Hollenberg

5f-1a: The University of Melbourne

5f-c: Corner of Swanston Street and Tin Alley

Melbourne VI 3010

5a: Frederick Green

5f-1a: The University of New South Wales

5f-c: CQCT, School of Physics

Sydney NS 2052

5a: Andrew D. Greentree

5f-1a: The University of Melbourne

5f-c: Corner of Swanston Street and Tin Alley

Melbourne VI 3010

5a: Alexander Rudolf Hamilton

5f-1a: The University of New South Wales

5f-c: CQCT, School of Physics

Sydney NS 2052

5 **Silicon single electron device**

Patent Filed in US? (5d-1) Y

Patent Filed in Foreign Countries? (5d-2) Y

Was the assignment forwarded to the contracting officer? (5e) N

Foreign Countries of application (5g-2): Australia

5a: Andrew Ferguson

5f-1a: The University of New South Wales

5f-c: CQCT, School of Physics

Sydney NS 2052

5a: Andrew Steven Dzurak

5f-1a: The University of New South Wales

5f-c: CQCT, School of Physics

Sydney NS 2052

5a: Robert Graham Clark

5f-1a: The University of New South Wales

5f-c: CQCT, School of Physics

Sydney NS 2052

5a: Susan Angus

5f-1a: The University of New South Wales

5f-c: CQCT, School of Physics

Sydney NS 2052

5 **Single molecule array on silicon substrate for quantum computer**

Patent Filed in US? (5d-1) Y

Patent Filed in Foreign Countries? (5d-2) Y

Was the assignment forwarded to the contracting officer? (5e) N

Foreign Countries of application (5g-2): Australia; China

5a: Michelle Yvonne Simmons

5f-1a: The University of New South Wales

5f-c: CQCT, School of Physics

Sydney NS 2052

5a: Steven Richard Schofield

5f-1a: The University of New South Wales

5f-c: CQCT, School of Physics

Sydney NS 2052

5a: Andrew Steven Dzurak

5f-1a: The University of New South Wales

5f-c: CQCT, School of Physics

Sydney NS 2052

5a: Jeremy Lloyd O'Brien

5f-1a: The University of New South Wales

5f-c: CQCT, School of Physics

Sydney NS 2052

5a: Robert Graham Clark

5f-1a: The University of New South Wales

5f-c: CQCT, School of Physics

Sydney NS 2052

5 **Solid state charge qubit device**

Patent Filed in US? (5d-1) Y

Patent Filed in Foreign Countries? (5d-2) Y

Was the assignment forwarded to the contracting officer? (5e) N

Foreign Countries of application (5g-2): Australia

5a: Lloyd Christopher Leonard Hollenberg

5f-1a: The University of Melbourne

5f-c: Corner of Swanston Street and Tin Alley

Melbourne VI 3010

5a: Andrew Steven Dzurak

5f-1a: The University of New South Wales

5f-c: CQCT, School of Physics

Sydney NS 2052

5a: Robert Graham Clark

5f-1a: The University of New South Wales

5f-c: CQCT, School of Physics

Sydney NS 2052

5a: Gerard J. Milburn

5f-1a: The University of Queensland

5f-c: 7 Cooper Road

St Lucia QL 4072

5a: David J. Reilly

5f-1a: The University of New South Wales

5f-c: CQCT, School of Physics

Sydney NS 2052

5a: Alexander Rudolf Hamilton

5f-1a: The University of New South Wales

5f-c: CQCT, School of Physics

Sydney NS 2052

5a: Cameron Wellard

5f-1a: The University of Melbourne

5f-c: Corner of Swanston Street and Tin Alley

Melbourne VI 3010

5 **Substituted donor atoms in silicon crystal for quantum computer**

Patent Filed in US? (5d-1) Y

Patent Filed in Foreign Countries? (5d-2) Y

Was the assignment forwarded to the contracting officer? (5e) N

Foreign Countries of application (5g-2): Australia

5a: Steven Richard Schofield

5f-1a: The University of New South Wales

5f-c: CQCT, School of Physics

Sydney NS 2052

5a: Lars Oberbeck

5f-1a: The University of New South Wales

5f-c: CQCT, School of Physics

Sydney NS 2052

5a: Toby Hallam

5f-1a: The University of New South Wales

5f-c: CQCT, School of Physics

Sydney NS 2052

5a: Neil Jonathan Curson

5f-1a: The University of New South Wales

5f-c: CQCT, School of Physics

Sydney NS 2052

5a: Robert Graham Clark

5f-1a: The University of New South Wales

5f-c: CQCT, School of Physics

Sydney NS 2052

5a: Michelle Yvonne Simmons

5f-1a: The University of New South Wales

5f-c: CQCT, School of Physics

Sydney NS 2052

# SOLID STATE QUANTUM COMPUTER IN SILICON

# CONTRACT NUMBER: W911NF-04-1-0290

# 1 July 2004 – 30 June 2008

ABSTRACT:

A Si:P electron-spin qubit architecture was developed in 2008, based upon research outcomes over the four-year QCCM grant. Single-shot spin readout will proceed via spin-dependent tunneling to a Si MOS rf-SET, which we have demonstrated to posses charge sensitivities equal to or better than Al rf-SETs. Spin manipulation will occur using local electron-spin resonance (ESR), which we have used to observe hyperfine-split electron spin resonances in P-doped Si MOSFETs. This spin qubit concept has been incorporated into the bi-linear array quantum computer design developed in parallel over 2004-2008 by the theory programs, which was one of the first quantum computer architectures quantitatively analyzed for the fault-tolerant threshold. Preliminary measurements on ion-implanted spin qubit devices have demonstrated transfer of P-donor electrons to a Si-SET detector with a large signal of ~0.2e, while tunneling structures have enabled transport spectroscopy of singly occupied (D0) and doubly occupied (D-) P-donor electron states. These measurements are strongly supported by the NEMO-TCAD program allowing donor species and position to be determined through transport spectroscopy. Single-ion implantation using on-chip PIN detectors now routinely produces Si:P devices with accurately positioned single donors, such as a 2-P-atom charge qubit device, in which electron transfer events and charge-state relaxation times have been measured. Using STM atom-scale lithography the narrowest conducting doped wires in silicon have been demonstrated and used to fabricate the first in-plane-gated dot architecture. Measurements of these dots highlight the stability of in-plane gates compared with top gates and provide a pathway to atomically precise single donor architectures. Ab-initio and self-consistent tight-binding approaches have made progress in describing the essential physics of these highly-doped nanostructures.

## SCIENTIFIC PROGRESS REPORT

CONTENT PAGE

# SCIENTIFIC PROGRESS - SOLID STATE QUANTUM COMPUTER IN SILICON

## A. FOREWORD

The Australian Research Council Centre of Excellence for Quantum Computer Technology (CQCT) was established in 2000 and has operated since then with significant funding from the ARO/NSA/ARDA-IARPA QC program as well as ongoing support from the Australian Research Council. Throughout this period CQCT has been led by the founding Director, Professor Robert Clark, and Deputy Director, Professor Gerard Milburn. The Centre represents the coordinated efforts of 170 staff and students across seven Australian and two US universities and institutions. Research is organized into ten experimental and nine theory programs (see chart), each led by a high-profile Program Manager, with areas of expertise encompassing nanofabrication and nanomaterials research, quantum semiconductor devices, ion beam physics, quantum optics and photon science, solid state theory, molecular dynamics, quantum theory of measurement and algorithms.

The QCCM grant (Contract No.: W911NF-04-1-0290) reported on here has supported the Centre's research in solid state quantum computing (SSQC) in silicon over the period July 2004 – June 2008. This research is based at the University of New South Wales (UNSW) and the University of Melbourne, with advanced atomistic modeling undertaken at Purdue University (USA) via a sub-contract of the QCCM grant. The QCCM grant has also supported the development of a visualization of the operation of a full-scale silicon quantum computer, partly through a sub-contract with the University of Calgary in Canada.

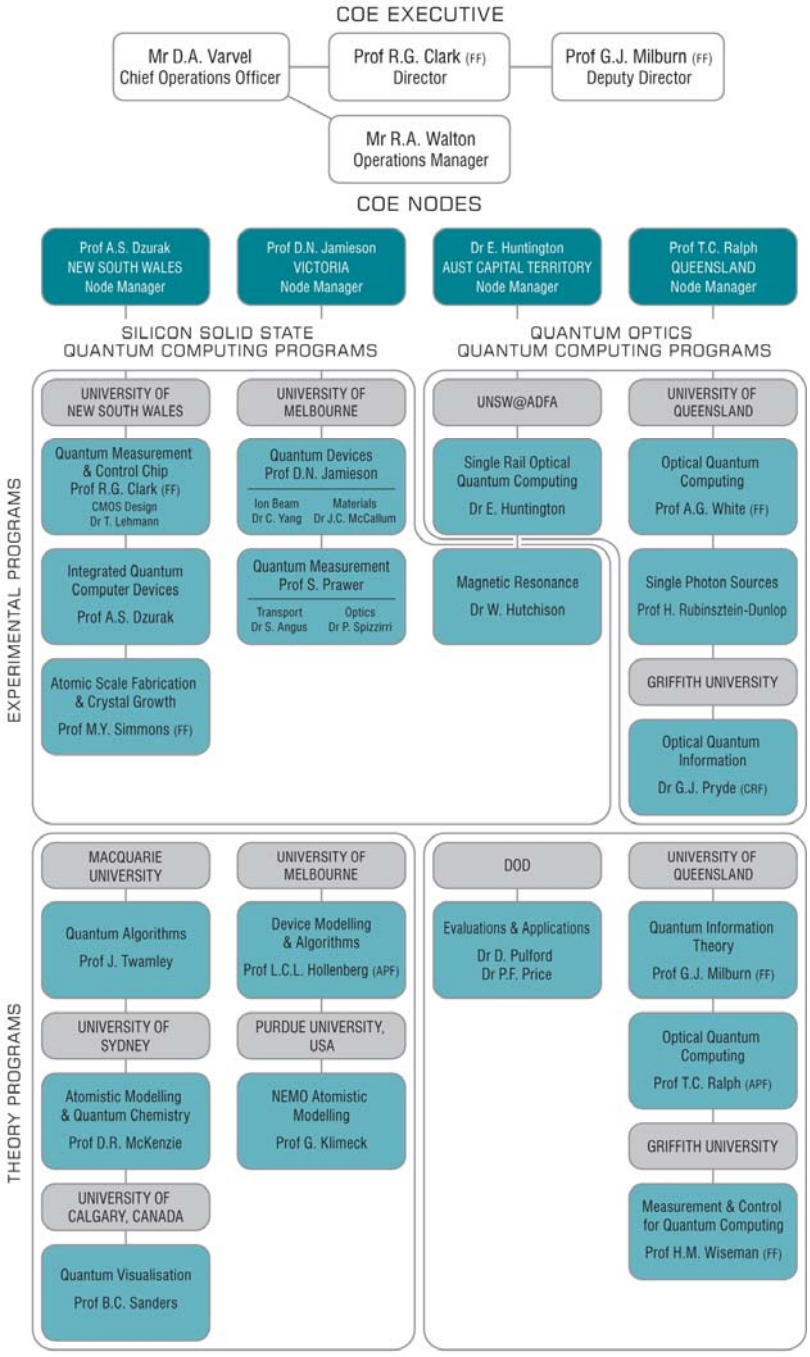


In addition to the international linkages supported via the QCCM grant, the Centre's research strengths are enhanced by active collaborations with over 50 national and international institutions. Collaborators within the US include Lawrence Berkeley National Laboratory, Los Alamos National Laboratory, the University of Wisconsin-Madison and the University of Maryland. Most significantly, in September 2008 the Centre signed a Cooperative Research and Development Agreement (CRADA) with Sandia National Laboratory to collaborate over the period 2008-2011 in the development of technologies for silicon-based quantum computing.

Throughout the term of the QCCM grant (2004-08) the Centre has produced 148 publications in peer-reviewed journals and delivered 251 presentations of research at international conferences, all in areas of relevance to solid-state quantum computation. A detailed listing of publications and presentations for the period August 2007-June 2008 is provided via the on-line report submitted with this scientific progress report.

## B. THE PROBLEM STUDIED: SILICON-BASED QUANTUM COMPUTING

Solid state qubit architectures, such as spins confined in lithographic quantum dots, spins of precisely-engineered shallow donors in semiconductors or Josephson junction qubits in superconducting circuits, are important due to the long coherence times of spin-based qubits, the scalability of solid state architectures and their compatibility with high speed classical control circuitry. In 1998, Kane proposed using the spin states of individual phosphorus dopant atoms in silicon as qubits. At the time it was widely believed that the realization of such a device was beyond the reach of nanotechnology for the foreseeable future. However, innovative atom-scale fabrication strategies developed in Australia held great promise and led to the formation of the Centre for Quantum Computer Technology (CQCT) in 2000 as an Australian Research Council Special Research Centre, with considerable support provided through ARO/NSA/ARDA-IARPA funding.

The original Kane scheme for a nuclear spin quantum computer in Si [1] and subsequent electron spin architectures [2,3] all rely on an ability to measure the state of a single electron spin associated with a phosphorus donor atom. Whilst demonstration of the control and readout of spin qubits is the Centre's ultimate goal, early milestones throughout the period of this QCCM focused on charge qubit devices, building on the Centre's existing fast rf-SET technology for single-shot charge read-out. This approach has provided an important test-bed for studies of electron transfer in few-P-atom Si:P nanostructures and has allowed characterization of the materials environment in Si:P MOS devices and their suitability for hosting single-donor spin qubits.

The Centre's research objectives have been pursued via two parallel approaches to qubit construction. The first involves a 'top-down' strategy in which counted single-ion implantation technology, combined with more conventional nanofabrication methods, allows the positioning of individual phosphorus dopants within the device. The second involves an atomic-precision 'bottom-up' strategy, which utilizes scanning probe technology to construct the qubit array atom-by-atom with atomic precision control of dopant location. Both approaches have delivered significant technological developments throughout the period of this QCCM, and have demonstrated the key components required for a spin qubit quantum computer architecture.

[1] B. E. Kane, Nature 393, 133 (1998).
[2] R. Vrijen et al., Phys. Rev. A 62, 12306 (2000).
[3] L.C.L. Hollenberg et al., Phys. Rev. B 74, 045311 (2006).

## C. STATEMENT OF KEY OUTCOMES FROM THIS GRANT

The goals of this QCCM grant have been pursued via coordinated experimental and theoretical efforts across programs at the University of New South Wales, the University of Melbourne and Purdue University. Key outcomes during the QCCM period August 2004 – July 2008 include:

- Demonstration of all key components for an MOS-compatible Si:P electron-spin qubit device, including local electron spin resonance (ESR) capability for coherent spin manipulation and Si-MOS rf-SETs for single-shot spin readout.
- Measurement of gate-controlled electron transfer from P donors to a Si-SET island in a Si-MOS spin qubit test device.
- Measurement of hyperfine-split electron spin resonances for phosphorus donor electrons in P-doped Si MOSFETs.
- Optimization of controlled single P-ion implantation techniques (incorporating advanced on-chip PIN detectors) and associated fabrication processes enabling the routine production of a range of Si:P devices containing one, two or larger clusters of phosphorus atoms.
- Measurement of extremely stable charge transfer events and charge state relaxation times of order 10 ms in a 2-P-atom charge qubit device.
- Measurement of charge transfer events and determination of the energy level structure of a 4-P-atom charge qubit device.
- Optimization of gate-oxide growth processes, achieving $Si/SiO_2$ interface trap densities $< 10^{10}$ $eV^{-1}cm^{-2}$.

- Demonstration of a complete atomically-precise fabrication route to scalable qubits using scanning probe microscopy, including donor alignment on one atomic plane, alignment of surface gates and incorporation of a low-temperature UHV compatible dielectric.
- Demonstration of the narrowest doped conducting wires in silicon, down to ~2nm thickness that still show ohmic conduction and very low resistivities. These wires have subsequently been incorporated into device architectures as *in-plane* gates, with nm precision alignment.
- Demonstration of an STM fabricated, all epitaxial *in plane* gated single electron transistor. By incorporating a surface gate on these devices we have been able to show that in the absence of the randomizing influences of interface and surface defects the electronic defect density in silicon is comparable or better than of quantum dots defined in other material systems
- Definition of a bi-linear array silicon quantum computer architecture based on the coherent transfer by adiabatic passage (CTAP) protocol, and analysis of fault-tolerant thresholds for its key operations.
- Integration of the NEMO tight-binding code with TCAD nanoelectronics simulation, providing the most sophisticated capability for donor-based quantum device simulation, and successful application to the modelling of key Si:P devices and experiments.

We now detail the key research outcomes for each of the programs supported via this QCCM grant for the period 2004-2008. While this report covers the entire 4-year period we focus, in particular, on results obtained within the past year, since the previous Interim Report (September 2007). The remainder of this report is presented in the following six sections, one for each of the key research program groupings:

D1. Atomic-scale Fabrication and Crystal Growth via STM/MBE
D2. Fast-Track Fabrication via Single-Ion Implantation
D3. Top-Down Device Fabrication, Quantum Measurement and Control Electronics
D4. Solid-State Device Modelling and Theory (including NEMO)
D5. Optical (Raman) Measurements
D6. Materials Research

# D. RESEARCH PROGRAMS

## D1. ATOMIC-SCALE FABRICATION AND CRYSTAL GROWTH VIA STM/MBE

**Key Achievements:** *Since the inception of the 4 year program we have now demonstrated the complete atomically precise fabrication route to scalable qubits, including the incorporation of a low temperature dielectric for gating, a first comparison of in-plane and surface gates, alignment of donors on one atomic plane and increased device yields to ~80%. Over the past year we have demonstrated the narrowest conducting doped wires in silicon and subsequently used these to fabricate the first in-plane gated dot architecture. The results from these dots highlight the stability of in-plane gate architectures compared with top gates and provide a pathway to atomically precise single donor architectures.*

Over the past 4 years we have completed the entire atomic-scale fabrication strategy based on using a combination of ultra-high-vacuum scanning tunnelling microscopy (STM) lithography and molecular beam epitaxy (MBE) growth to fabricate scaleable arrays of P qubits in Si (Figure 1.1) [1-16]. We have optimised the fabrication process to attain device yields of ~70-80% by transferring all the *ex-situ* fabrication steps from optical to EBL lithography [17], and have increased alignment of surface contacts to buried STM-patterned layers to below ~50nm. Using EBL-defined circular makers (Figure. 1.2a,b) we can create atomically flat plateaus for accurately positioning donors on a single atomic Si plane (Figure 1.2c,d). We have also demonstrated the fabrication of homogeneous low temperature silicon dioxide dielectric shown in the cross sectional TEM micrographs (Figure 1.3a,b) [18].

Despite the low temperature of formation of the oxide we find we can apply several volts to the gate before leakage and have used this to gate buried quantum dot devices patterned by the STM, see Figure 1.3c,d. Electrical characterization at 4 K show non-linear I-Vs with blockaded transport and the occurrence of several equidistant electron resonances indicative of resonant transport either through the energy levels of the dot or resonant levels within the tunnel barriers. Variation of the top gate results in a clear modulation of the conductance gap reminiscent of Coulomb blockade.

We have since gone on to investigate the use of STM-patterned regions as *in-plane-gates* as shown in Figure 1.4a,b. Operating this device as a three-terminal dot shows non-linear electron transport through the dot in which one of the terminals can be used as an in-plane gate to modulate the conductance gap. This method has the potential to provide the highest alignment capability as devices reach the atomic level. To further investigate this, over the past year we have investigated conduction in ultra-thin wires – down to 2 or 3 dimers wide [19-21].

Figure 1.5(a,c) shows STM images of a 2nm wide wire, where we can see the dimer rows. The I-V characteristics of these devices show linear, ohmic behaviour with resistivities a factor of 10-100 lower than other techniques Figure 1.5(b,d). These low values are indicative of the absence of surface states close to the wires and the high carrier densities they contain. Interestingly these devices also show signs of containing just one conductive mode.

Extensive work has been completed on understanding the incorporation chemistry of P dopants in silicon at these small device lengths [23-29] and their effects on the conductance of devices [30-37]. The width of the wires has also found to be crucial in the ability to modulate the conductance across tunnel gaps – an essential part of any device.

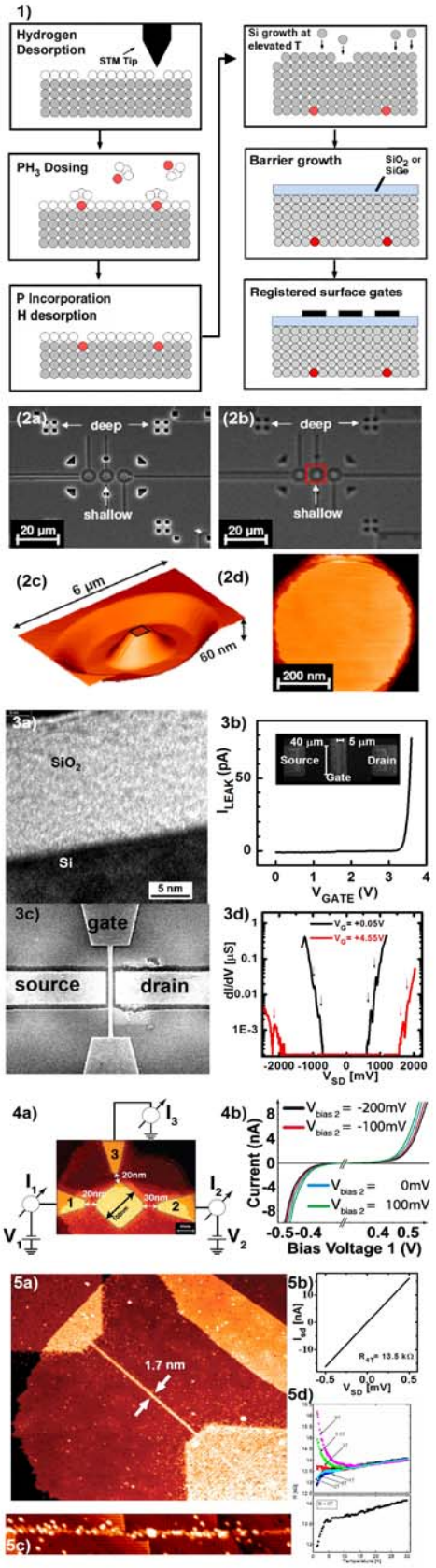


Figure 1: (1-3a,b) Completion of atomically precise fabrication route to scalable silicon qubits.; (3c,d) Measurement of gated STM fabricated devices using top gates and (4a,b) in-plane gates; 5(a-d) demonstration of the narrowest conducting doped wires in silicon – only 2-3 dimers wide with good ohmic conduction.

We have fabricated a series of tunnel gaps [38] with different lengths, see Figure 1.6(a-c) and have found that the conductive gap is very sensitive to the device geometry. In particular we see we can modulate the width of the gap controllably by changing the separation of the source-drain leads, but even more important is the width of the leads. In Figure 1.7 we compare the same length tunnel gap but with different width of source-drain lead. We can clearly see that the gap is considerably higher with thinner leads. This is consistent with devices where we have made ordered dopant arrays, see Figure 1.8. By pulsing the STM tip we can pattern dots approximately 6nm in diameter, with ~50 P atoms in each dot between source-drain leads [39]. We observe a large gap in the conductance with a minimum threshold voltage of ±250 mV caused by the ordering of the dopants.

From the many devices we have fabricated over the past 4 years we have now designed and fabricated quantum dot devices towards the atomic level, using the knowledge gained. In Figure 1.9 we show the first *in-plane* gated quantum dot device [40], where in plane regions of highly doped silicon can be used to gate quantum dots resulting in highly stable Coulomb blockade oscillations. In particular we compare the use of these all epitaxial in plane gates (Figure 1.10b) with conventional surface gates (Figure 1.10a) and find superior stability of the former. These results show that in the absence of the randomizing influences of interface and surface defects the electronic defect density in silicon is comparable or better than of quantum dots defined in other material systems.

These experiments are currently being pursued towards the single donor limit, where work is currently underway to observe spin dependent transport through single donors, Figure 1.11.

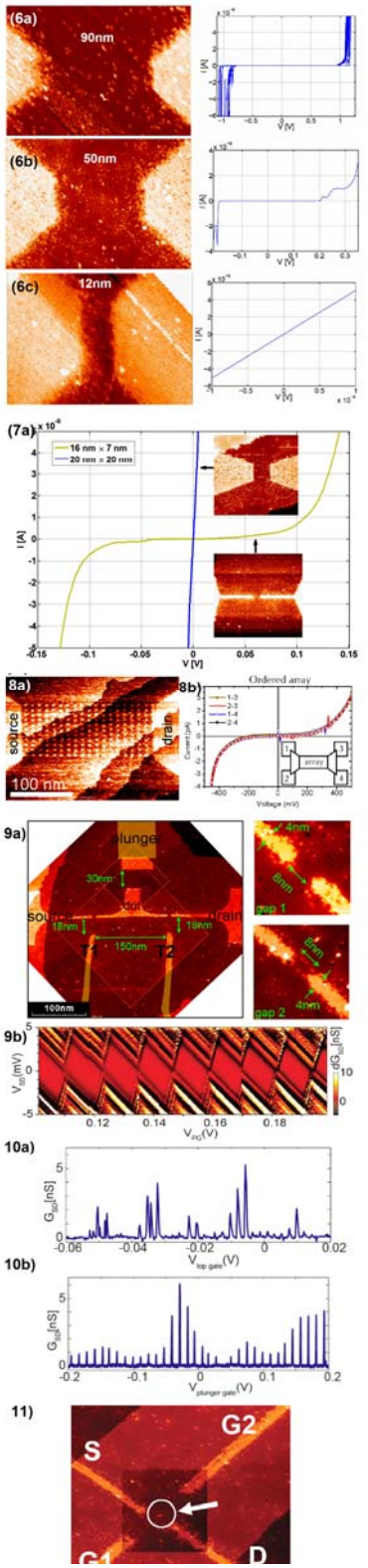


Figure 1: (6,7) Importance of channel geometry on height of conductance barrier in STM-fabricated devices; (8) Demonstration of ordered dopant arrays with 5nm dots containing ~50 P donors separated by ~10nm; (9,10) first all epitaxial *in-plane* gated single electron transistor showing stability of in-plane gates compared with top gates and (10) the use of in-plane gates towards the single donor limit.

**Bibliography**


[1] F.J. Rueß *et al.*, Nano Letters 4 (10), 1969-1973 (2004).
[2] L. Oberbeck *et al.*, Applied Physics Letters 85, 1359 (2004).
[3] K.E.J. Goh *et al.*, Applied Physics Letters 85, 4953 (2004).
[4] L. Oberbeck *et al.*, Thin Solid Films 464, 23-27 (2004).
[5] F.J. Rueß *et al.*, Nanotechnology 16, 2446 (2005).
[6] M.Y. Simmons *et al.*, Mol. Sim. 31, 505(2005).
[7] K.E.J. Goh *et al.*, Phys. Stat. Sol. A 202, 1002 (2005).
[8] T. Hallam *et al.*, Appl. Phys. Lett. 86, 143116 (2005).
[9] O. Warschkow *et al.*, Phys. Rev. B 72, 125328 (2005).
[10] G.W. Brown *et al.*,Physical Review B 72, 195323 (2005).
[11] K.E.J. Goh *et al.*, Physica Status Solidi A 202, 1002 (2005).
[12] K. E. J. Goh *et al.*, Phys. Rev. B 73, 035401 (2006).
[13] S. R. Schofield *et al.*, J. Phys. Chem. B 110, 3173 (2006).
[14] T. C. G. Reusch *et al.*, Surf. Sci. 600, 318 (2006).
[15] M. W. Radny *et al.*, Physical Review B 74, 113311 (2006).
[16] H.F. Wilson *et al.*, Physical Review B 74, 195310 (2006).
[17] M. Fuechsle *et al.*, J. Vacuum Science and Technology B 25, 2562 (2007).
[18] G. Scappucci *et al.*, Applied Physics Letters 91, 222109 (2007).
[19] F.J. Ruess *et al.*, Small, 3, No. 4, 563-567 (2007).
[20] F.J. Ruess *et al.*, Nanotechnology 18, 044023 (2007).
[21] F. J. Rueß *et al.*, Physical Review B 76, 085403 (2007).
[22] F. J. Rueß *et al.*, Applied Physics Letters 92, 0521011 (2008).
[23] M.W. Radny *et al.*, Physical Review B 76, 155302 (2007).
[24] M.W. Radny *et al.*, J. Chemical Physics 127, 184706 (2007).
[25] T.C.G. Reusch *et al.*, J. Phys. Chem 111, 6428 (2007).
[26] T.C.G. Reusch *et al.*, Surface Science 601, 4036 (2007).
[27] T.C.G. Reusch *et al.*, J. Appl. Phys 104, 066104 (2008).
[28] T. Hallam *et al.*, Journal of Applied Physics 101, 034305 (2007).
[29] T. Hallam *et al.*, Journal of Applied Physics 102, 034308 (2007).
[31] M.Y. Simmons *et al.*, Int. J. Nanotechnology 5, 352 (2008).
[32] M.Y. Simmons, Nature Physics 4, 165 (2008).
[33] K.E.J. Goh *et al.*, Nanotechnology 18, 065301 (2007).
[34] K.E.J. Goh *et al.*, Physical Review B 76, 193305 (2007).
[35] K.E.J. Goh *et al.*, Phys. Rev. B 77, 235410 (2008).
[37] F.J. Rueß *et al.*, Physical Review B 75, 121303(R) (2007).
[38] F.J. Rueß *et al.*, Physica E 40, 1006 (2008).
[39] W. Pok *et al.*, Nanotechnology, IEEE Transactions on, 6 (2), 213-217 (2007).
[40] A. Fuhrer *et al.*, Manuscript in preparation (2008).

## D2. FAST-TRACK FABRICATION VIA SINGLE-ION IMPLANTATION

**2004-2008 highlights.** The successful development of a reliable method for controlled single ion implantation into devices has led to a process flow compatible with the routine production of quantum computer devices containing one, two or larger clusters of phosphorus atoms. As documented elsewhere in this report, these devices have exhibited a rich array of phenomena consistent with controlled single electron transfers between the implanted donors and represent important milestones on the path to a Si:P quantum computer. Building on these accomplishments, strategies have been developed to address the even larger challenge of building a qubit transport device that again employs controlled single ion implantation for fabrication. These transport devices are prototypes for a comprehensive 2D scalable architecture [1] which employs single phosphorus atoms in silicon, which can act as charge or spin qubits, together with arrays of single P atoms designed to implement the Charge Transport by Adiabatic Passage (CTAP) protocol [2].

**Routine single ion implantation for a few donor devices (2004-2008).** In collaboration with the Integrated Quantum Computer Device Program the standard single ion implantation process (see Figure 2.1) is in routine use to fabricate arrays of devices containing one or two counted atoms [3] (see Figure 2.2). These devices take advantage of the long electron spin coherence [4], and the negligible spin-orbit coupling possible in isotopically pure $^{28}$Si to ensure extremely long relaxation times. The strategy employs a pure silicon substrate (>$10^4$ Ωcm) masked with a polymethylmethacrylate (PMMA) film patterned with Electron Beam Lithography and the implanted ions are counted by the signal induced in on-chip detector electrodes from the ionization created as the ions come to rest inside the substrate.

The method employs the PIN detector electrode structure introduced in 2005 and further refined in 2006 in order the noise threshold of the on-chip detectors to improve the confidence level of the process. Each implant will liberate about 1000 e-/h+ pairs which drift in the internal electric field and induce a transient charge on the electrodes of duration 500 ns as calculated [5] using modelling packages for ion implantation SRIM (Simulation of ranges of ions in matter, www.srim.org) and semiconductor devices TCAD (Technology Computer Aided Design, Integrated Systems Engineering AG, Zurich, http://www.ise.com).

We have also continuously developed the chip packaging technique for the substrates to overcome significant noise issues associated with standard semiconductor chip carriers. Our package for the samples with on-chip PIN detectors employs a customised ceramic backing and wire-bond pads optimised for low capacitance.

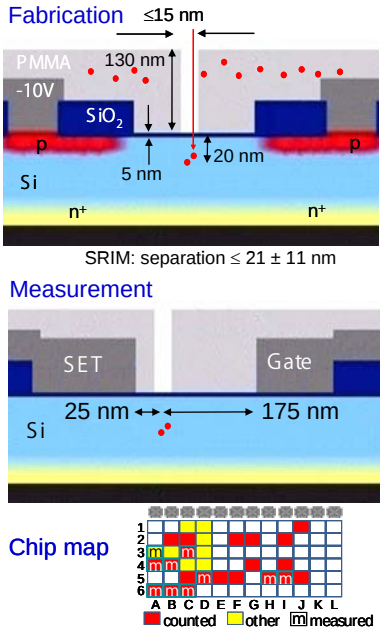


Figure 2.1: Single ion implantation schematic for 14 keV $^{31}$P ions, schematic of device post patterning with control and readout nanocircuitry and chip map of implants for a production run to fabricate many devices.

**Colutron single ion implantation extension to step-and-repeat (2008).** Building on the successful implementation of the single ion implantation method, the Centre has made significant progress in the technical development of the step-and-repeat system toward the precision fabrication of single atom arrays in a silicon substrate for CTAP (see Figure 2.4) which employs adiabatic tunnelling to transport single phosphorus donor electron spin qubits along arrays of charged P donors from storage sites to interaction sites. Construction of the CTAP test device requires placing single phosphorus donor atoms into a silicon device with a sub-20 nm precision. The architecture of the device must also allow control and readout of the qubits. Our architecture includes MOS gate-induced 2DEG reservoirs [6] for spin-dependent tunneling from a single P donor, together with the integration of local electron spin resonance for coherent spin manipulation with a silicon single electron transistor [7] detector for spin readout. Most importantly, the fabrication process flow for the construction of these important ancillary components is compatible with controlled single ion implantation [8] of the Si:P components.

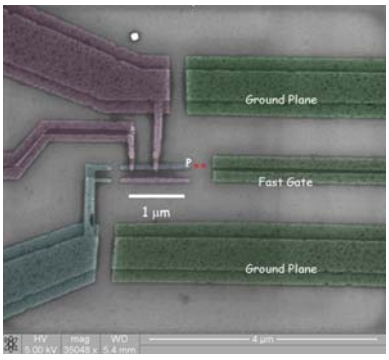


Figure 2.2: Qubit test device with two counted atoms and nanocircuitry for control and readout.

We have concluded that the optimum near-term route to arrays of more than two atoms will be via a scanned nano-stencil fabricated using Focused Ion Beam (FIB) machining (see Figure 2.3). After a series of workshops held with our collaborators in the Centre and beyond, the design for a sub-50 nm high precision step-and-repeat system for 14 keV P ion implantation has been devised. The system is now under construction and incorporates an attocube stack that will be used to scan a nano-stencil cantilever drilled to high precision with our FIB system and narrowed by backfilling with Pt. Precision localisation of the implanted atom is accomplished by the use of a scanned nano-stencil and a substrate incorporating a nanoaperture machined by a focused ion beam system and associated alignment markers. These precision fabrication tools have already been used to demonstrate ion beam lithography [9] with the nano-stencil to a precision of better than 30±10 nm (see Figure 2.5), with higher precision possible in the near future.

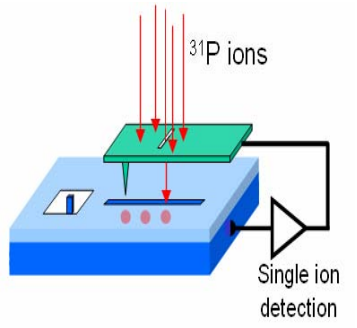


Figure 2.3: Step and repeat concept with scanned nanostencil.

**Detector technology development – MOS versus PIN versus A-PIN (2004-2005).** The development of reliable single ion implantation passed through several stages of detector improvements [10]. Prototype devices were imaged by use of the Ion Beam Induced Charge (IBIC) analysis method, employing a scanned, focused microprobe of 2 MeV alpha particles. This technique measured the charge collection efficiently of different detector architectures including MOS and PIN structures which were then optimised for keV single ion detection. The PIN detector structure was revealed by IBIC maps to have a charge collection efficiency 100% at the construction site between the detector electrodes over a wide range of bias voltages (10-40 V).

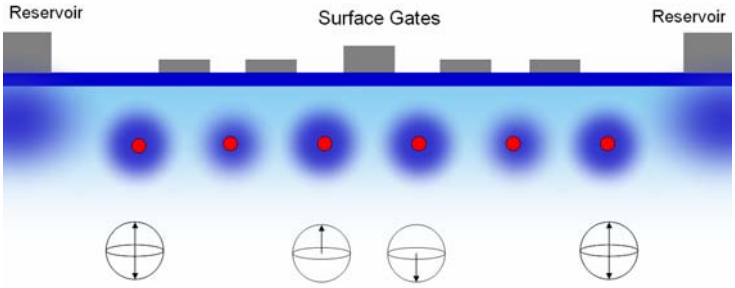


Figure 2.4: CTAP concept with adjoining three atom chains. Red dots represent single $^{31}$P atoms buried beneath a gate oxide. Inter-atom spacing is nominally 20 nm.

**Development of avalanche high accuracy single ion detectors (2007-2008).** We have explored the development of the detector technology to accomplish the detection of phosphorus ions implanted at lower energy than the present 14 keV where the effects of straggle are reduced to allow higher precision placement. A promising method is to use high internal electric field to induce avalanche charge multiplication following ion impact. This gives higher signals for low energy ion implants. By use of the IBIC method, this idea was tested with a commercially available avalanche photodiode which revealed that the avalanche process significantly multiplies the signals from ion impacts [11]. We are presently developing methods of integration of an avalanche process into our detectors which will allow us to reliably implant lower energy ions. We have done computer simulations of these results and have developed a design which incorporates an avalanche layer into our existing p-i-n structure to achieve a charge gain exceeding a factor of 10.

**Cluster ion implantation for single dots and QCA devices (2006-2007).** The successful operation of a single quantum dot [12-14] and multiple quantum-dot cellular automata (QCA) have been demonstrated. The QCA cell was based on four $^{31}$P ion implanted quantum dots and self-aligned leads [15]. The devices are configured with four independent control gates and two SETs which monitor charge transfer within the four dot cell to assess the coupling strength between the dots. The ion implantation for this class of device was accomplished by timed charge integration of the ion beam incident on the sample which provided sufficient accuracy for the required fluence. Other classes of devices have been fabricated using this method including electrodes separated by narrow barriers in which tunnelling occurs through straggled ions [16]. Simulations have also been performed on the potential of implanting with $P_2^+$ molecular ions for the fabrication of self-aligned two atom devices [17] and this technique may be employed in the future.

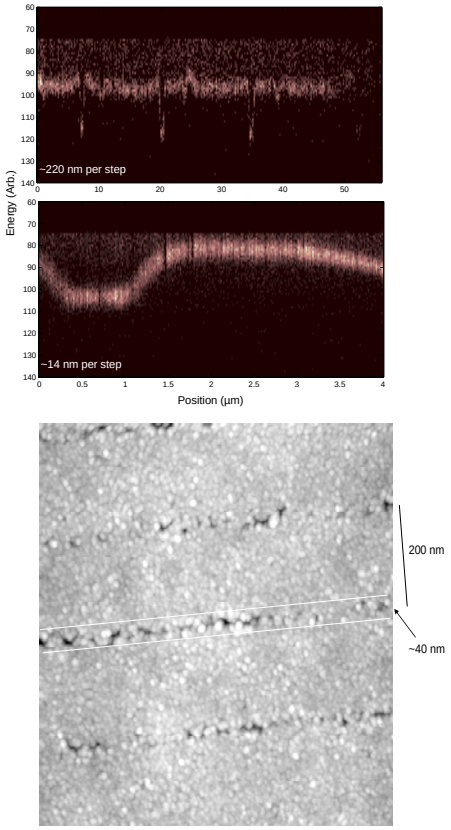


Figure 2.5: (top) Demonstration of single ion implantation through a nanoscale EBL test mask at sub-30 nm resolution. (bottom) Ion beam lithography with a sub-30 nm wide nanostencil in PMMA.

**Ion strike positioning by coincidence IBIC measurement (2006).** At present, our single ion counting method does not provide any information about the location of the ion strike on the substrate. In the fabrication of devices containing three atoms in a row, or larger arrays, spatial information would allow us to identify optimum devices even without the ability to target specific sites in the substrate. Our strategy of counting single ion strikes by collecting the signals induced in on-chip electrodes offers a potential development for identification of the position of the ion strike. By using two or more independent electrodes, the signals from each electrode could be used to measure the position of an ion strike on the substrate. To test this strategy in 2006 some of our standard devices were configured with independent detector electrodes and wired to independent data acquisition systems. This allowed us to perform IBIC experiments to investigate the charge collection of individual electrodes. These experiments were performed using a focused microprobe of 2 MeV alpha particles, produced by the 5U Pelletron accelerator at the University of Melbourne and the MP2 nuclear microprobe system. The results show that the charge is shared between the two electrodes in proportion to the position of the ion strike as expected. This result is supported also by TCAD simulations and verifies the possibility of identifying the ion strike position from the electrode signals. At present we are investigating the possibility of using this result to identify the ion strike position for 14 keV $^{31}P$ ions used in our devices.

**TCAD Modelling of Device Structures (2004-2008).** Technology Computer Aided Design (TCAD) simulations have been carried out in parallel with the experimental work on the development of the single-ion detector architectures. These simulations helped us to understand the role of contact and wafer doping on the device leakage current and charge collection efficiency for single implanted ions. This is a major ongoing study. The TCAD models also feed into the Centre's Device Modelling program where the TCAD potentials are used in a full quantum mechanical simulation of the devices.

**Highly Charged Ions (2006).** In collaboration with Dr Thomas Schenkel of the Lawrence Berkeley Laboratory (LBL) in California, we applied our single ion detection method to study the energy deposition of highly charged ions in our detectors. Our PhD student Toby Hopf made an extended visit to LBL to perform the necessary experiments. The results indicated that highly charged ions with a kinetic energy of less than 100 keV dissipate the potential energy due to their high charge state within 5 nm of the surface. This suggests the implantation of highly charged ions offers a way of depositing large amounts of ionisation to the surface of a substrate. The data also suggest that highly charged ions experience a much higher stopping power compared to singly charged ions. It is possible that because of this highly charged ions also have lower straggling and hence higher spatial precision compared to singly charged ions. However the high potential energy of highly charged ions did not result in a higher ion impact signal compared to singly charged ions.

---

**Bibliography**


[1] L.C.L. Hollenberg *et al*., Phys. Rev. B 74, 045311 (2006).
[2] A.D. Greentree *et al*., Phys. Rev. B 70, 235317 (2004).
[3] D.N. Jamieson *et al*., Appl. Phys. Lett. 86, 202101 (2005).
[4] A.M. Tyryshkin *et al*., Phys. Rev. B 68, 193207 (2003).
[5] T. Hopf *et al*., Nucl. Instr. Meth. in Phys. Res. B 231: 463-466 (2005).
[6] S.J. Angus *et al*., Appl. Phys. Lett. 92, 112103 (2008).
[7] S.J. Angus *et al*., Nano Lett. 7, 2051 (2007).
[8] J.A. Van Donkelaar *et al*., arXiv:0806.2691v1 [quant-ph] (2008).
[9] V. Millar *et al*., Nanotechnology 16, 823-826 (2005).
[10] C. Yang *et al*., Proc. Int. Conf. on Nanoscience and Nanotechnology (ICONN 2006) Brisbane Convention and Exhibition Centre July 3-7 2006.
[11] C. Yang *et al*., Proc. 15th AINSE Conference on Nuclear and Complementary Techniques of Analysis & 10th Vacuum Society of Australia Congress, 21 – 23 November 2007, Melbourne, Australia, ISBN0975843427.
[12] V.C. Chan *et al*., J. Appl. Phys. 100 (10) Art. No. 106104 (2006).
[13] T.M. Buehler *et al*., Appl. Phys. Lett., 88, 192101 (2006).
[14] F.E. Hudson *et al*., Microelec. Eng. 83 (4-9): 1809-1813 (2006).
[15] M. Mitic *et al*., Appl. Phys. Lett. 89, 013503 (2006).
[16] D.N. Jamieson *et al*., Nucl. Instr. Meth. In Phys. Res B249, 221-225 (2006).
[17] H.F. Wilson *et al*., Nucl. Instr. Meth. In Phys. Res B251 395-401 (2006).

## D3. TOP-DOWN DEVICE FABRICATION, QUANTUM MEASUREMENT AND CONTROL ELECTRONICS

**MOS Spin-Qubit Architecture (2008).** One of the Centre's most significant recent achievements has been the development of a MOS-based spin-qubit architecture (Figure 3.1) which brings together key capabilities developed throughout the 2004-2008 QCCM period [1]. Formally defined in January 2008, this scaleable architecture combines the following features:

*i) Accurately positioned P donors:* As detailed in section D2, single ion counting techniques developed in the Centre [2] are now a mature technology with on-chip PIN detectors delivering 100% charge collection efficiency and implantation through nanometre scale resist masks forming part of a well-defined Si:P device fabrication process [3,4].

*ii) Coherent spin manipulation via microwave fields:* The effective operation of our local electron spin resonance (ESR) lines for spin control has been demonstrated in electrically-detected magnetic resonance (EDMR) measurements on Si-MOS devices with few implanted donors [5]. In the spin qubit architecture, coherent manipulation of the qubit state will be achieved by applying controlled microwave pulses to the ESR line to induce Rabi oscillation of the spin state. In addition, the electrostatic potential on the ESR line is used to shift the Zeeman-split electron spin levels with respect to the Fermi level of the reservoir.

*iii) Single-shot readout via Si rf-SETs:* Spin-to-charge conversion is obtained when the Fermi level of the reservoir is half-way between the ground (spin-up) and excited (spin- down) electron spin states, allowing the qubit state to be read by single-shot detection of charge transfer. Since the electron tunnels directly onto the SET island, the magnitude of the charge transfer signal is expected to be very large, of order 10% of an electron, which is easily detectable by our Si rf SETs [6].

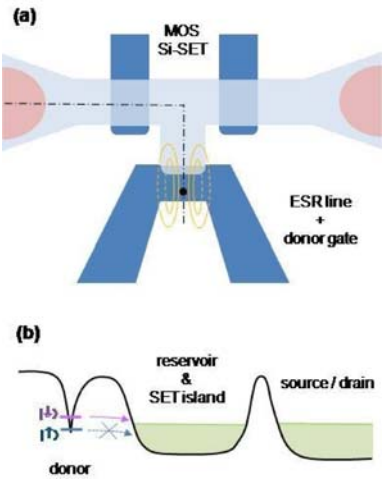


Figure 3.1: (a) Sketch of complete device for control and readout of the electron spin of a single P donor. The Si-SET has an extended island that protrudes towards the donor site. An additional metal gate provides both the local microwave excitation and the DC bias to lift the donor state. (b) Energy landscape along the dash-dotted line shown in panel (a). Notice that the island of the SET acts also as a reservoir for the spin-dependent electron tunnelling to and from the donor.

**Electrically Detected Magnetic Resonance (EDMR): Spin Qubit Control (2007-08).** A systematic EDMR study of ion-implanted Si:P devices with as few as 100 P donors was reported by the Centre in 2006 [7]. During 2007, we designed devices (Figure 3.2a) where a topgate in the form of a coplanar transmission line, terminated by a short circuit serves the double function of i) inducing a 2DEG in the MOSFET channel, and ii) supplying the microwave field. The ability to perform local ESR on a small number of donors was demonstrated in broadband EDMR measurements of P-doped Si MOSFETs, and for the first time, this type of investigation was extended into the mK regime where the spin polarisation of P donors is expected to be very high [5]. The measured spectra (Figure 3.2b) reveal hyperfine-split electron spin resonances and structure attributed to spin-spin scattering in the 2DEG.

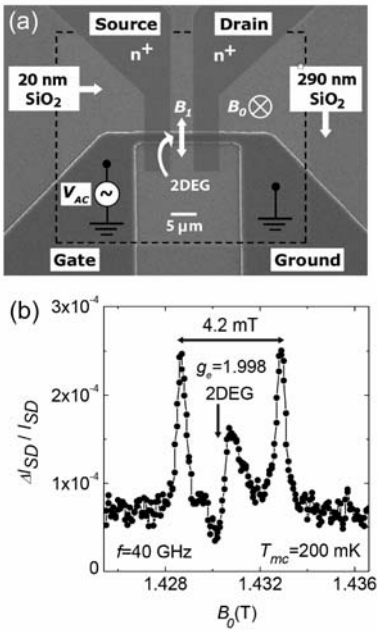


Figure 3.2: (a) SEM image of a MOSFET used for EDMR. (b) EDMR spectrum obtained by magnetic field modulation at f=40 GHz using P=100 mW.

**Si Quantum Dots and Si rf-SET: Fast Spin Qubit Readout (2006-08).** The Centre's development of a fully MOS-compatible multi-layer Al gating technology in 2006 led to the fabrication of Si quantum dots with tuneable barrier gates (Figure 3.3a,b) allowing the dot to be either strongly or weakly coupled to its leads. In addition, the top gate can be used to control the number of electrons in the dot. Figure 3.3e shows bias spectroscopy of a dot with only ~10 electrons, exhibiting clear evidence of discrete energy levels within the quantum dot [8]. Due to the large charging energy of such a dot, connection to a resonant LC tank circuit (Figure 3.3c) allows operation of the dot as a highly sensitive rf-SET. Demonstration measurements of a not yet optimised Si rf-SET achieved a charge sensitivity of order 10 $\mu E/\sqrt{Hz}$ at 2 MHz [6], on par with the performance of mature Al rf-SET technology. This excellent sensitivity enables measurement of a charge transfer equivalent to 1% of an electron, with a measurement time of ~1 µs.

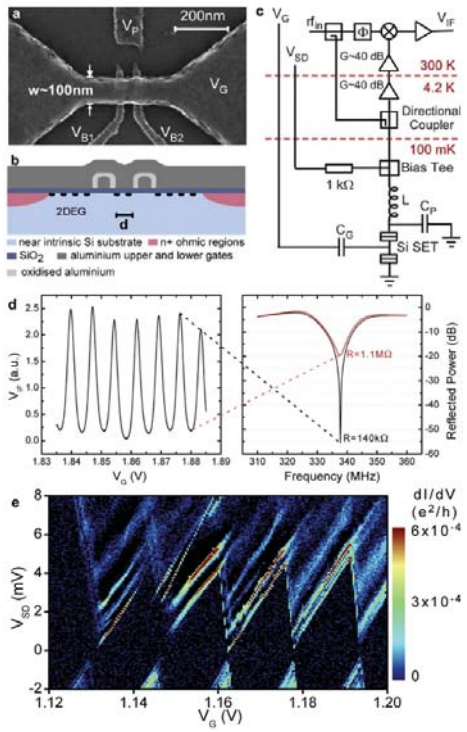


Figure 3.3: Silicon rf SET. (a) SEM image and (b) schematic cross-section of a device (c) Schematic of rf-measurement set-up (d) When operated in a tank circuit, the Coulomb blockade peaks (left) are obtained from the modulation of the reflected microwave power (right) as a function of top gate voltage. The charge sensitivity achieved by biasing the device on the steepest slope of the coulomb peaks is better than 10 μe/√Hz (e) DC bias spectroscopy on a similar device, with gate width w=50 nm, biased to a regime with only ~10 electrons in the dot. Excited states in the dot are clearly evident.

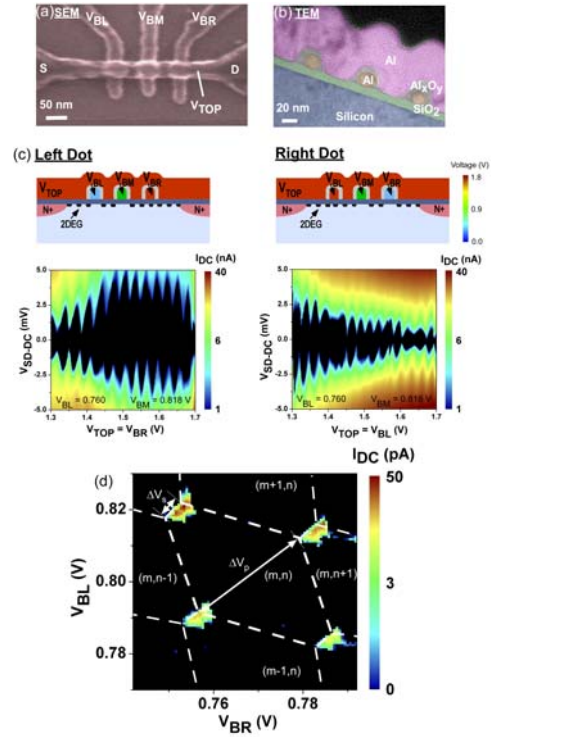


Figure 3.4: (a) SEM image of Si double quantum dot structure. (b) Colour-enhanced TEM image through top gate showing cross-section of three electrically isolated barrier gates. (c) Independent characterization of left and right dots. (d) Bias spectroscopy of coupled double-dot system.

**Si Double and Triple Dots: Towards CTAP (2007-08).** In 2007, the Centre's Si quantum dot studies were extended to fully tuneable double quantum structures (Figure 3.4). We performed transport measurements to individually characterise each dot, and demonstrate the ability to tune the device through a wide range of inter-dot coupling strengths. Bias spectroscopy provided evidence of excited states in the few electron regime [9]. The extension of these studies to Si triple quantum dot devices provides a test-bed for scale-up via the recently proposed coherent transfer by adiabatic passage (CTAP) protocol [10].

**Cryogenic rf-CMOS Pulse Generators: Classical Control Electronics (2004-08).** The development of classical CMOS control electronics to interface with silicon-based qubit structures has been progressing throughout the period of this QCCM. Control pulse generator circuits (Figure 3.5) with low power dissipation have been designed, fabricated and tested at cryogenic temperatures in both a mixed mode and a digital design [11].

**Implanted Si:P Cluster Devices (2004-06).** In order to characterise the Si:P material system and develop the fabrication technology required to build Si:P qubits, early studies in the 2004-2008 QCCM period explored devices with clusters of implanted P atoms. In large single dots (containing tens of thousands of P atoms), the observation of Coulomb blockade consistent with charging of a single metallic dot demonstrated the success of implantation and surface gating processes. The incorporation of SETs for charge detection allowed the full characterisation of both inter-dot and dot-lead charge transfer events, and demonstrated gate control of the central tunnel barrier from the extreme of single dot behaviour through a wide range of inter-dot coupling regimes [12,13].

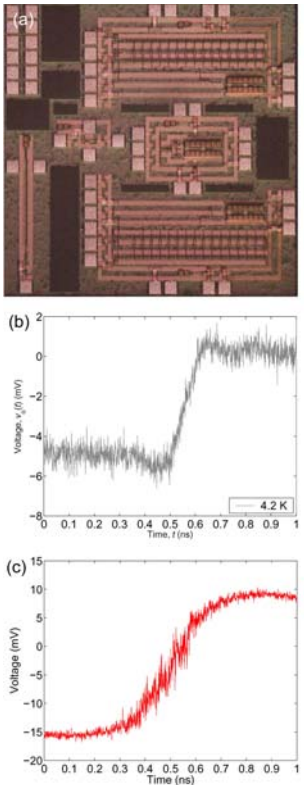


Figure 3.5: (a) Optical micrograph of second generation voltage pulse generator. Control pulse outputs from (b) first generation mixed mode design and (c) second generation digital design.

Further refinements to fabrication and implantation processes achieved a significant reduction in dot size. Inter-dot charge transfer was first observed in isolated double dot structures (around 30 nm diameter dots each containing 600 P atoms) with no source or drain leads [14]. With leads incorporated, we were able to correlate transport and SET charge detection leading to further insights into single [15] and double [16] dot systems.

Studies of Si:P cluster devices reached a culmination in 2005 when the operation of the basic cell of a quantum cellular automata (QCA) was demonstrated [17]. The QCA cell comprised two pairs of P-implanted dots, with SETs incorporated as charge transfer detectors (Figure 3.6). With electron tunnelling only possible between dots within a pair, gate voltage-driven inter-dot tunnelling in pair A was shown to induce a reverse electron transfer in pair B.

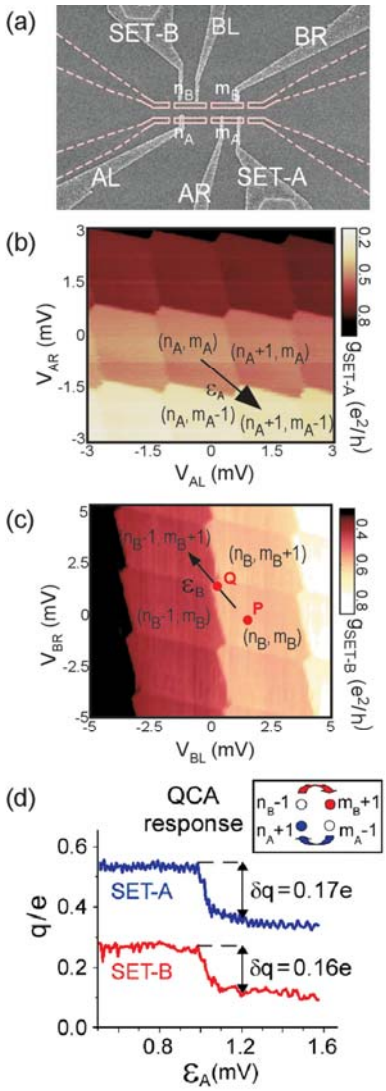


Figure 3.6: (a) SEM image of Si:P quantum cellular automata (QCA) device with four (buried) ion-implanted P dots and two (surface) readout SETs. Charge stability data for (b) the lower and (c) the upper pair of P dots. (d) Demonstration of a QCA bit flip.

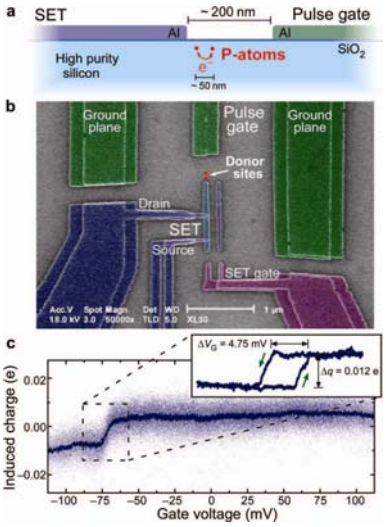


Figure 3.7: (a) Schematic and (b) colour-enhanced SEM image of 2-P-Atom device. (c) Induced charge on SET island, measured at MHz bandwidth for several gate sweeps with averaged data in solid. Inset of averaged charge transfer shows hysteresis in gate voltage.

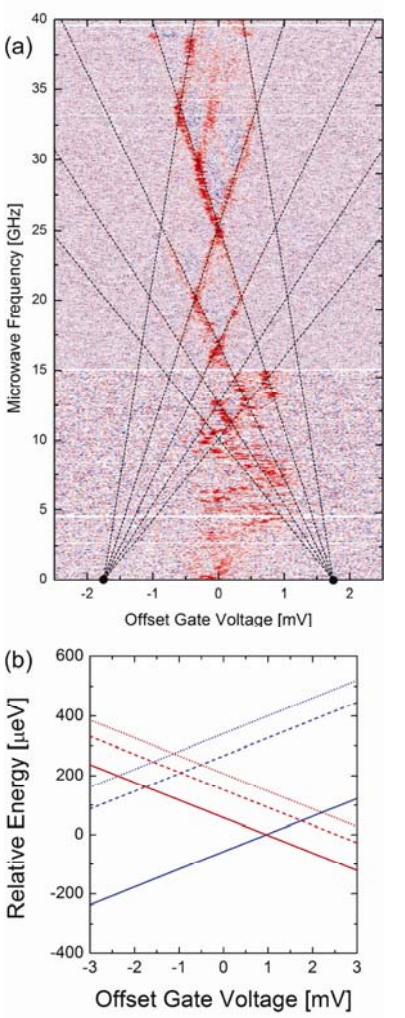


Figure 3.8: 4-P-Atom device. (a) SET signal as a function of applied gate voltage and applied microwave frequency. Dotted lines are a fit to theory. (b) Energy levels of the $(P_3\text{-}P)^{2+}$ system.

**Charge Qubit Devices (2004-06).** As a stepping stone towards the goal of spin-based qubits, early research during the 2004-2008 QCCM period focussed on the controlled manipulation and readout of charge qubits [18]. One of the highlights from this research [19] was the first conclusive measurement of single electron transfer in an atomically-engineered Si:P device performed at the Centre on a silicon device with exactly two implanted P donors (Figure 3.7). Time resolved measurements on this system incorporated fast pulsing of the local electrostatic potential and rf-SET detection [20-22], revealing extremely stable charge transfers and charge state relaxation times of order 10 ms.

Microwave spectroscopy of devices with four implanted P atoms provided the first measurement of the energy level spectrum of a donor-molecule system in Si (Figure 3.8). The device used in these measurements comprised four P atoms implanted through two nanoscale apertures, individually detected by on-chip single-ion detectors. Charge transfer events between components of the 4-P-Atom system were detected using an rf-SET [20-22], and microwave spectroscopy revealed multi-phonon excitation spectra from which an energy level spectrum consistent with a $(P_3\text{-}P)^{2+}$ system (ie $P_3$ 'molecule' and single P, 50 nm apart, with only two electrons) was derived.

**Quantum-Limited Electrometry (2004-07).** The Centre's advanced capability in quantum-limited electrometry [6, 20-27] is built upon our Al-$Al_2O_3$ rf-SETs [20-25] which have been successfully employed in many studies of quantum devices throughout the Centre's history. Studies of quasiparticle transport in nanoscale superconducting devices [28] have led to the production of Single Cooper Pair transistors (SCPTs) which hold great promise as low-noise, low-dissipation electrometers of quantum systems. SCPTs rely upon the coherent tunnelling of a single Cooper pair between a reservoir and a tunnel-coupled island. However the supercurrent is blocked, and SCPT operation limited by quasiparticle poisoning: the incoherent tunnelling of quasiparticles onto the island. The Centre's detailed studies of quasiparticle poisoning events allowed the quasiparticle temperature to be determined [29] and revealed a process for reducing quasiparticle poisoning. In band-structure-engineered superconducting films [30,31], we were able to reduce quasiparticle poisoning by up to three orders of magnitude and resolve 2e-periodic supercurrent peaks.

**Single P Atom MOS Tunnelling Devices (2008).** Since the MOS-based architecture was defined in January 2008, a series of resonant tunnelling devices has been fabricated and measured to demonstrate various aspects of the planned spin qubit devices (Figure 3.9). The first of these transport devices [32] comprised single tunnel junctions on bulk-doped Si substrates. Weak conductance peaks attributable to P donors under the barrier gate were observed, however strong conductance fluctuations (most likely related to electron scattering from dopants in the 2DEG) dominated the data (Figure 3.10a-b).

In a second series of devices [32] based on intrinsic Si, controlled ion implantation through a PMMA mask allowed small numbers of P donors (typically 2, 3 or 4) to be accurately located in the active region of the device (i.e. beneath the overlap of top gate and barrier gate). With the conductance fluctuations observed in bulk-doped devices eliminated, data from locally doped devices clearly map tunnelling through states below the conduction band (Figure 3.10e-h), with stronger coupling apparent in devices implanted at lower energy. The absence of these transport signatures in measurements of control samples with no P implants (Figure 3.10c-d) provides strong evidence that donor states are being probed in implanted devices. Most recently, the observation of Zeeman shifts of possible donor levels in an applied magnetic field (Figure 3.11) has allowed identification of $D^0$ and $D^-$ states.

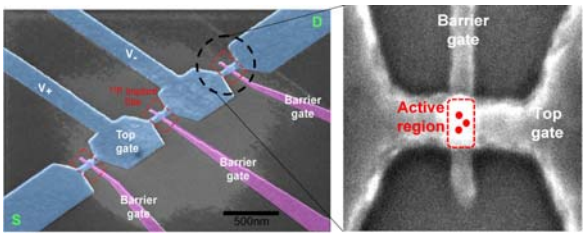


Figure 3.9: SEM images of MOS tunnelling devices. The image to the left shows a tribarrier design which allows three independent single barrier tunnelling measurements to be performed on each device.

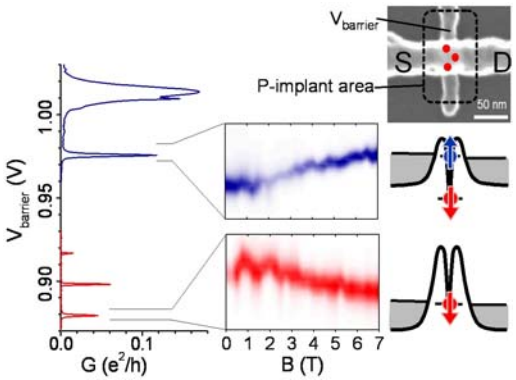


Figure 3.11: Bias spectroscopy of MOS tunnelling device with three implanted donors, showing Zeeman shifts of electron states associated with individual donors.

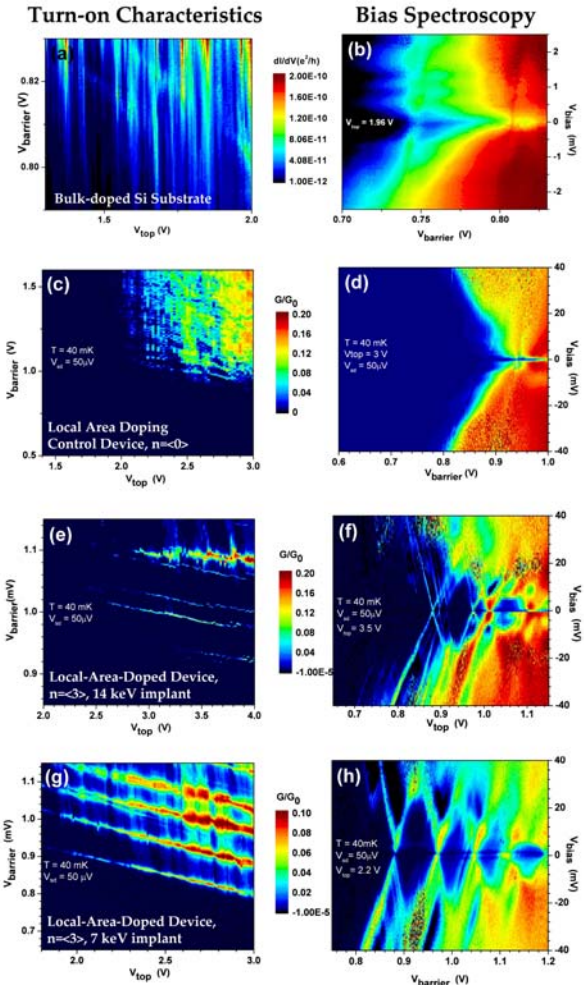


Figure 3.10: Turn-on characteristics (left) and bias spectroscopy (right) for MOS tunnelling devices fabricated on (a-b) bulk-doped Si, (c-h) i-Si substrates. (c-d) is for a local area doping control device with no implanted donors. (e-f) is for a local area doped device with three donors implanted at 14 keV. (g-h) is for a local area doped device with three donors implanted at 7 keV.

**Single P Atom Spin Qubit Devices (2008).** In parallel with studies of MOS transport devices described above, a series of spin qubit devices has been fabricated combining local P donor implants and Si rf-SETs (Figure 3.12). Operation of the SET as a charge sensor has been confirmed in preliminary measurements of these devices. Charge transitions in the Coulomb peaks of the SET are induced as donor energy levels are altered as a function of plunger gate voltage. Capacitance modelling predicts that signature features of gate voltage characteristics will allow charge transitions to be identified with specific donor locations in the device. Following this interpretation, the set of charge transition pairs observed in preliminary electrical measurements is consistent with the nominal P donor configuration. Ongoing measurements incorporating spin dependent readout and magnetic resonance techniques seek to unequivocally identify interactions with P donors.

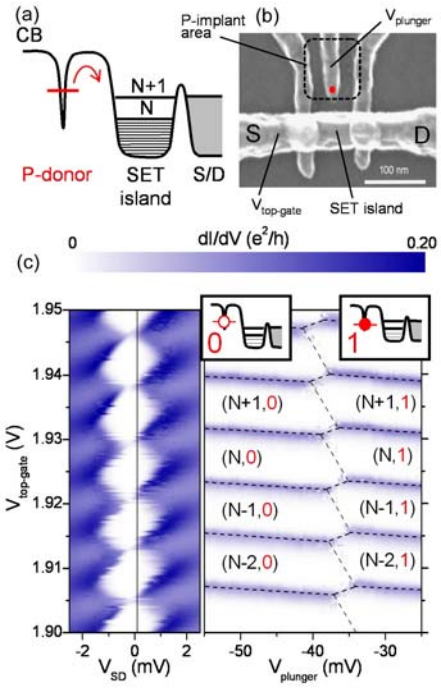


Figure 3.12: (a) Energy landscape and (b) SEM image of locally doped Si:P MOS device with SET island acting as induced electron reservoir. (c) Voltage spectroscopy of the device reveals individual single electron transfers from P-atom to SET island.

## Bibliography


[1] A. Morello *et al*., to be submitted to Phys. Rev. B.
[2] D.N. Jamieson *et al*., Appl. Phys. Lett. 86, 202101 (2005).
[3] M. Mitic *et al*., Microelectronic Engineering 78-79, 279 (2005).
[4] C.C. Escott *et al*., Nanotechnology 18, 235401 (2007).
[5] L.H. Willems van Beveren *et al*., Appl. Phys. Lett. 93, 072102 (2008).
[6] S.J. Angus *et al*., Appl. Phys. Lett. 92, 112103 (2008).
[7] D.R. McCamey *et al*., Appl. Phys. Lett. 89, 182115 (2006).
[8] S.J. Angus *et al*., Nano Lett. 7, 2051 (2007).
[9] W.H. Lim *et al*., to be submitted to Appl. Phys. Lett.
[10] J.H. Cole *et al*., Phys. Rev. B 77, 235418 (2008).
[11] S.R. Ekanayake *et al*., submitted to IEEE Transactions on Electron Devices.
[12] V.C. Chan *et al*., J. Appl. Phys. 100, 106104 (2006).
[13] M. Mitic *et al*., Nanotech. 19, 265201 (2008).
[14] T.M. Buehler *et al*., Appl. Phys. Lett. 88, 192101 (2006).
[15] F.E. Hudson *et al*., Microelectronic Engineering 83, 1809 (2006).
[16] F.E. Hudson *et al*., Nanotech. 19, 195402 (2008).
[17] M. Mitic *et al*., Appl. Phys. Lett. 89, 13503 (2006).
[18] L.C.L. Hollenberg *et al*., Phys. Rev. B 69, 113301 (2004).
[19] S.E. Andresen *et al*., Nano Letters 7, 2000 (2007).
[20] T.M. Buehler *et al*., J. Appl. Phys. 96, 4508 (2004).
[21] R. Brenner *et al*., J. Appl. Phys. 97, 34501 (2005).
[22] R. Brenner *et al*., Microelectronic Engineering 78-79, 218 (2005).
[23] T.M. Buehler *et al*., Appl. Phys. Lett. 86, 143117 (2005).
[24] D.J. Reilly and T. M. Buehler, Appl. Phys. Lett. 87, 163122 (2005).
[25] A.J. Ferguson *et al*., Appl. Phys. Lett. 88, 162117 (2006).
[26] M.J. Biercuk *et al*., PRB 73, 201402 (2006).
[27] M. Cassidy *et al*., Appl. Phys. Lett. 91, 222104 (2007).
[28] A.J. Ferguson *et al*., Phys. Rev. Lett. 97, 86602 (2006).
[29] A.J. Ferguson *et al*., Phys. Rev. Lett. 97, 106603 (2006).
[30] N.A. Court *et al*., Phys. Rev. B 77, 100501 (2008).
[31] N.A. Court *et al*., Superconductor Science and Technology 21, 15013 (2008).
[32] K.Y. Tan *et al*., to be submitted to Nano Letters.

## D4. SOLID STATE DEVICE MODELLING AND THEORY (INCLUDING NEMO)

**2004-2008 highlights:** Over the past 4 years the theory program has achieved and exceeded many of the program milestones in device modelling and architecture development. Highlights include: development of the bi-linear array silicon quantum computer architecture based on CTAP transport and associated analysis of the fault-tolerant thresholds for concatenated logical CNOT and T-gate under the Steane code, the silicon quantum computer visualization project, complete integration of the NEMO tight-binding code with TCAD nanoelectronics simulation providing the most sophisticated capability for donor based quantum device simulation (charge and spin qubits and CTAP devices), precision benchmarking of modelling against key experiments (charge and spin), linear-nearest-neighbour implementation of Shor's algorithm, quantum control and characterization techniques for precision CNOT gates mitigating atomic-level fabrication errors, and engagement with engineering and systems design realities for full scale quantum computer development.

**2007-2008 key achievements:** *NEMO simulation of gated donor system verifying hybridization of donor-interface states observed in transport spectroscopy, a new message passing algorithm which improves concatenation scaling of quantum error correction, Density Functional Theory applied to highly doped Si:P systems for STM device modelling, capability to analyse high-threshold surface codes, robust control techniques for exchange based CNOT gates in the presence of charge noise.*

**Fault-tolerant threshold of the bi-linear silicon quantum computer.** Practical quantum computer design, requires more than just qubits and interactions, it requires a full analysis of all of the parameters necessary to operate fault-tolerantly. Most importantly, this means that multiple levels of quantum error correction must be able to be performed, which is an extremely stringent demand. In 2006 we began an analysis of the fault-tolerant properties of an implementation of the proposed 2D donor electron spin architecture – the bi-linear array shown in Figure 4.1. This architecture was also the subject of a significant scientific visualisation project associated with the QCCM project (Figure 4.2). We specifically compiled the DiVincenzo-Aliferis quantum error correction protocol for the Steane code on the bi-linear array: scheduling transport, gate and measurements steps (Figure 4.3). We calculated lower bounds to the CNOT pseudo thresholds for increasing concatenation levels (Figure 4.4). We find lower bounds for the asymptotic threshold in the range $10^{-8}$ – $10^{-6}$, which depend on the times and fidelities for gate, transport and measurement. These calculations are significant as they constitute significant steps towards the fault-tolerant and design analysis of a silicon quantum computer architecture. Recent work has concentrated on the prospects for improving thresholds using alternative codes and QEC techniques, and in achieving such stringent thresholds in physical devices.

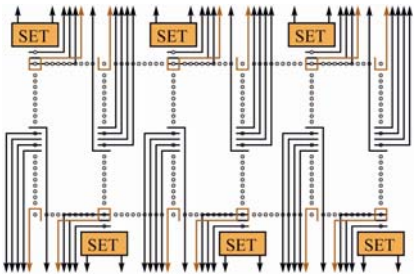


Figure 4.1: Bi-linear Si:P array with horizontal and vertical transport rails into and out of central interaction regions.

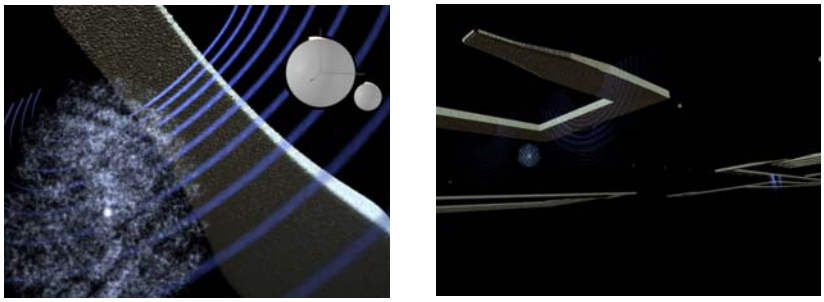

Figure 4.2: Scenes from the silicon quantum visualization project (EDM studios).

**Quantum device modeling.** In the period 2004-2008 a great deal of effort was directed towards the modelling milestones for both charge and spin based qubit systems, as well as CTAP transport devices. In particular, a major effort was directed towards the integration of the NEMO tight-binding capability at Purdue with the TCAD based band-minima basis methods developed in the CQCT program. This work has culminated in several significant successes with atomistic quantum descriptions of Si:P donor qubit systems (NEMO tight-binding and band minima basis) integrated with TCAD nanoelectronic simulation capability now tested against experiment to high precision. NEMO simulations have also been carried out on a CTAP 3-atom device demonstrating theoretically the transport control pathway for realistic donor systems.

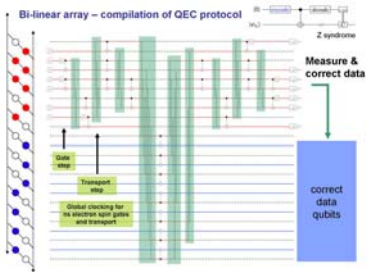


Figure 4.3: Compilation of the DiVincenzo-Aliferis QEC protocol (Z-syndrome shown) for the Steane code on the bi-linear array showing gate and transport schedules. Compounding such protocols for X and Z syndrome extraction into the extended rectangle for encoded gates (e.g. CNOT) and subsequent concatenation allows for the determination of a lower bound of the fault-tolerant thresholds (pseudo and asymptotic).

In the past year, the description of orbital Stark shifts under surface gate fields has been verified against transport spectroscopy data for As donors in close proximity to the Si-SiO2 interface [1] (Figure 4.5). Further benchmarking of donor qubit device modelling against key experiments has been carried out for spin control (hyperfine [2] and g-factor Stark shift). This capability paves the way for detailed simulations of MOS based donor qubit devices simulated underpinning CQCT experiments.

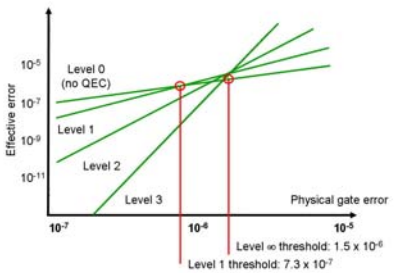


Figure 4.4: Error thresholds (lower bounds) for the encoded CNOT gate at various levels of concatenation, showing pseudo-thresholds (Level 1 = 7.3 x $10^{-7}$) and asymptotic threshold estimate (Level ∞ = 1.5 x $10^{-6}$) for a conservative set of inputs with respect to physical times and error rates for gates, transport and measurement.

**Message passing in fault tolerant quantum error correction.** Since the bi-linear concept and associated threshold analysis was carried out, work has been directed to the improvements of the stringent requirements. A fertile ground area is not just in the choice of QEC code, but in the QEC process itself. Classical information obtained from quantum error correction can be used to estimate the probability of a logical error. This information can be used to improve higher levels of error correction. Whenever a non-zero syndrome is observed at the physical level, the position in the circuit is flagged at the level above as having an increased likelihood of error on the encoded qubit (Figure 4.6). These flags can be used to determine the cause of any higher level syndromes more accurately than standard QEC techniques. For two levels of error correction this results in a reduction of the logical failure rate relative to conventional error correction by a factor proportional to the reciprocal of the physical error rate [3].

**Highly doped Si:P structures.** In addition to the large body of work in single and few donor devices, we have turned our attention in the past year to the more challenging case of the highly doped Si:P structures fabricated in the bottom up program. Two approaches are being pursued: self-consistent tight-binding (Purdue), and Density Functional Theory (Melbourne and SNL).

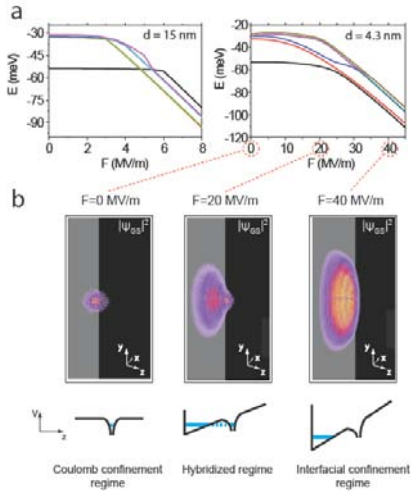


Figure 4.5: a) Stark shift of donor orbital levels as a function of field strength and donor depth. b) Hybridization of donor states near an interface: NEMO calculations used to interpret experimental data.

Work has progressed to compute the electronic charge bound to impurities self-consistently as an electrostatic potential through Poisson's Equation coupled with the atomistic Schoedinger equation. First prototypes were created in Matlab for later integration into NEMO3D and our new code base OMEN. OMEN combines the transport capabilities of NEMO1D and the electronic structure capabilities of NEMO3D.

We have simulated regular strings of impurities embedded into a Si nanowire and computed charge self-consistently the dispersion of that P-impurity nanowire. The nanowire cross section was quite small of 2x2nm$^2$. We observe (Figure 4.7) a downshift of 60meV in the carrier dispersion due to the insertion of P impurities compared to the ideal nanowire. This is a good trend where in experiments a 50-70meV barrier was observed between a heavily doped P impurity array and a pure Si buffer. We plan to implement the charge-self-consistent calculation into OMEN which will ultimately replace the NEMO3D code base.

Using the software package CRYSTAL06 [4] we have modelled bulk Si:P as a precursor to modelling STM nanostructures. Our all-electron basis (modified from [5]), and our effective core potential and valence basis sets (modified from [6, 7]), gave lattice parameters within 0.08Å of the true value (+1.5%). Preliminary calculations have been carried out of the donor level for Towler silicon and Harrison [8] phosphorus basis sets (at 8.5% H-F mix) for 64 and 216 atom systems. Using Effective Core Potentials (pseudopotentials) to model the core electrons reduces the number of basis functions required, giving an order of magnitude reduction in the calculation runtime.

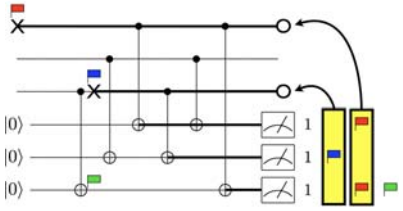


Figure 4.6: Message passing: flags raised by the first level of error correction are tracked through the circuits of the second level of error correction to aid in the diagnosis of level-1 errors. In this example, the blue and red flags match the measured syndrome and are thus identified as being the most likely errors.

**Topological surface code quantum computing.** Topological quantum computing on the two-dimensional surface code requires only local interactions between qubits yet allows long distance logical operations and can tolerate a physical error rate of up to one percent. [9, 10]. Logical qubits are created by introducing defects into the surface and logical operations are performed by applying chains of local operations and measurements. In the past year we have carried out numerical simulations of a single defect – a single logical qubit – on a surface to verify the threshold error rate (Figure 4.9) and to explore the application of such codes to the silicon system.

**Precision CNOT with fabrication and noise errors.** Composite pulse approach to mitigating variations in exchange coupling J(V) allows for precise CNOT gates [12]. In the past year, the effect of random noise fluctuations in the exchange strength due to charge noise was considered in the context of robust control techniques and fabrication errors. The system is initially modelled as an Ising interaction disturbed by a random telegraph noise process (RTN) in the superoperator formalism. Apart from an expected opaque fidelity window at the gate time scale, the robust CNOT gate clearly outperforms the uncorrected gate (Figure 4.10).

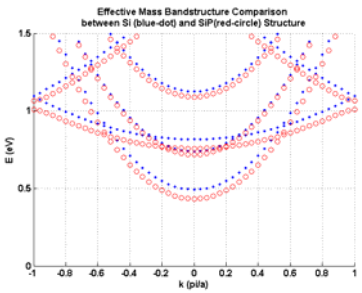


Figure 4.7: Dispersion of a 2x2nm$^2$ nanowire with and without centrally embedded line of P atoms. A 60meV downshift due to the insertion of the P impurities can be observed.

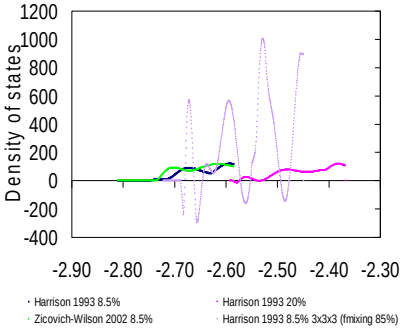


Figure 4.8: Density of states at the top of the bandgap for varied supercell sizes, phosphorus basis sets and Hartree-Fock mixing parameters. The Harrison P basis set and 8.5% H-F gives the dopant level at 62.6meV (64 atom) and 34.5meV (216 atom).

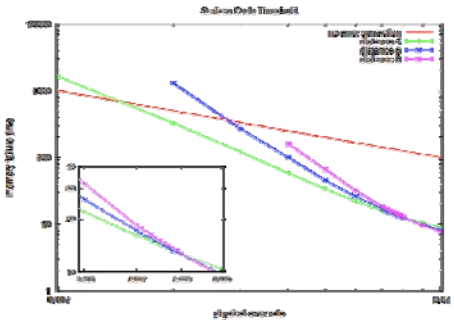

Figure 4.9: Average number of time steps before logical failure plotted for several surface distances. The threshold is defined to be the physical error rate below which arbitrarily long failures times can be reached by increasing the distance of the surface. As seen in the inset, the threshold error rate is around 0.0075 close to the original calculations [9].

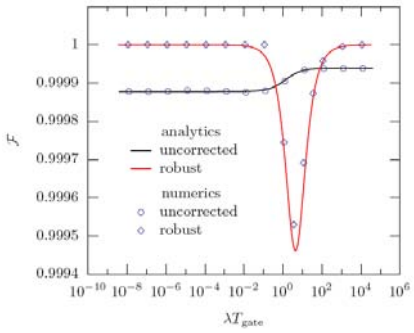


Figure 4.10: CNOT gate fidelity as a function of RTN rate λ for the uncorrected and robust gates when a small amount of uncertainty (1%) exists in the coupling strength. The results show that the robust gate now clearly outperforms the uncorrected gate in both the small and large λ limits. This suggests that although the composite rotations are designed to correct for static errors, in a noisy system which is not perfectly characterised, using the composite rotations to construct robust gates may be advantageous.

## Bibliography


[1] R. Rahman *et al.*, Phys. Rev. Lett. 99 036403 (2007).
[2] G. Lansbergen *et al.*, Nature Physics 4, 656 (2008).
[3] Z. Evans and A. Stephens, arXiv:0806.2188 [quant-ph].
[4] R. Dovesi *et al.*, CRYSTAL06 User's Manual (2006).
[5] A.R. Porter *et al.*, Phys. Rev. B 60(19), 13534 (1999).
[6] P. Durand & J.-C. Barthelat, Theoret. Chim. Acta 38, pp 283-302 (1975).
[7] Y. Bouteiller *et al.*, Molecular Physics 65 (2), pp 295-312 (1988).
[8] CRYSTAL Resource Page www.tcm.phy.cam.ac.uk/~mdt26/crystal.html.
[9] R. Raussendorf and J. Harrington, Phys. Rev. Lett. 98, 190504 (2007).
[10] A. Fowler, A. Stephens, and P. Groszkowski, arXiv:0803.0272 [quant-ph].
[11] W. Cook and A. Rohe, INFORMS J. Comput. 11, 138 (1999).
[12] M. Testolin *et al.*, Phys. Rev. A 76 012302 (2007).

## D5. OPTICAL (RAMAN) MEASUREMENTS

**2004-2007 Research Program Highlights:** Over the past 4 years, the Optical Measurement Program has developed spectroscopic technologies to study the material properties that underpin an all silicon QC architecture. In addition to developing the optical techniques necessary to observe donor wavefunction overlap (i.e. exchange coupling), some selected research highlights for this period include:

(i) Developing donor placement strategies using low energy ion implantation techniques.

(ii) Providing critical analysis of silicon device interfaces with atomic resolution (i.e. FIB prepared TEM analysis of device structures).

(iii) Surface terminations that allow ESR analysis of low (10keV < E < 20keV) and very low energy $P^+$ implants (< 5keV) to study donor activation and exchange effects.

(iv) Providing feedback to the device fabrication program about the quality of the materials being used.

**2007-2008 Key Achievements.** The Optical (Raman) Measurement program has been working on the spectroscopic analysis of phosphorus doped silicon including ion implanted ensembles with a view to understanding: (i) lattice defects arising from the phosphorus ion implantation process, (ii) the influence of interface states on donor ionisation, (iii) phosphorus donor-donor interactions and (iv) the influence of the local electronic environment on donor level spectroscopy. The key achievements of this program during 2007-08 have included the observation of: residual (silicon) lattice damage following ion implantation, donor ionisation arising from defected interface states (i.e. Si-$SiO_2$) and phosphorus donor-donor interactions from ion implanted phosphorus ensembles.

**Far Infra-Red (FIR) Absorption Spectroscopy of Ion Implanted Ensembles.** The spectroscopy of impurity atoms located in an elemental silicon host lattice has a long history with the archetypal system of Si:P extensively investigated. In this study, we report on one method of analysing for the impurity, namely far-infrared magneto-spectroscopy [1]. Since absorption spectroscopy is sensitive to the total number of absorbing centres through which the beam passes, we can calculate the equivalent two-dimensional density of P atoms in bulk (control) samples and compare this with the assumed two-dimensional density of the ion implanted ensembles. The samples prepared for this study are listed in Table 5.1 and include ion implanted ensembles, a highly bulk doped sample of Si:P and a neutron transmutation doped (NTD) control sample of Si:P.

| | SiPRL3A | SiPB | SiP4 | SiP5 |
|---|---|---|---|---|
| doping | bulk | bulk | implanted | implanted |
| details | NTD | 0.1 Ω-cm | 16 keV $P_2$ | 180 keV |
| thickness ($\mu$m) | 1588 | 262 | 333 | 326 |
| $n_{3D}$ (cm$^{-3}$) | $1 \times 10^{14}$ | $8 \times 10^{16}$ | – | – |
| $n_{2D}$ ($10^{12}$ cm$^{-2}$) | 16 | 2096 | 5 | 100 |

Table 5.1. Summary of the Si(P) samples.

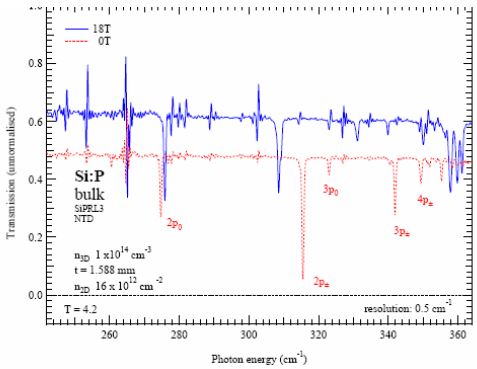


Figure 5.1. Spectrum of a "lightly" doped sample of Si(P) in both zero magnetic field (bottom, dashed, red line) and in magnetic field of 18T (top, full, blue line).

Measurements at 0T and 18T magnetic fields from the lightly doped (NTD) and heavily bulk doped ([P] = 8x10$^{16}$ cm$^{-3}$) samples are shown in Figures 5.1 and 5.2 where the donor transitions (i.e. 1*s* ground state to excited states) are apparent. Note that the very sharp lines in the spectra are due to water vapour and the application of a magnetic field causes the lines to shift and split as is evident from the spectrum shown at 18 T. The "heavily" doped sample in Figure 5.2 exhibits much deeper and broader lines in transmission arising from concentration broadening and a change in the ionisation energy with doping. From the areal ($n_{2D}$) donor densities, signal from the implanted samples should be similar in intensity to that of the NTD control sample however as is evident in Figures 5.3 and 5.4, the two ion-implanted samples do not exhibit any transitions associated with excitation from the 1s state of P in Si.

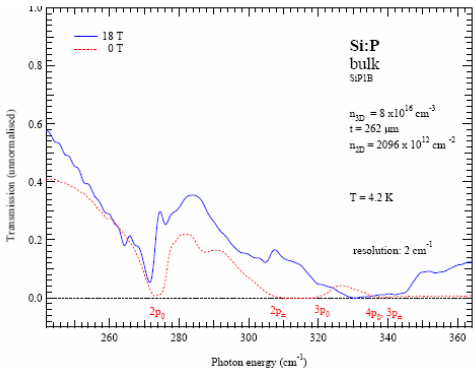


Figure 5.2. Spectrum of a "heavily" doped sample of Si(P) in both zero magnetic field (bottom, dashed, red line) and in magnetic field of 18T (top, full, blue line).

Possible explanations for the lack of observed lines in the implanted substrates include: imperfect P substitution on the host lattice or residual lattice damage following the high temperature anneal or a combination of these factors. Ionised donors arising from localised charged traps (lattice imperfections) can also result in a diminished P signal and is considered a likely cause in this work.

**Electron Spin Resonance Spectroscopy of Ion Implanted Ensembles.** Throughout 2008, work has continued using electron spin resonance (ESR) to study dopant activation and interfacial oxide defects. Electron spin resonance is an ideal technique for probing Si:P spin qubits and metering the success of the implantation and activation processes. It can also be used to study donor-donor interactions (i.e. exchange coupling) arising from various implantation strategies including the use of molecular $P_2^+$ ion beams. However, previous work [2] has shown very low ESR signal recovery from implanted ensembles, possibly reflecting reduced donor activation for low (i.e. <20 keV) energy implants. In this work [3], we have returned to a very fundamental scenario and report on the application of ESR to measurements of phosphorus implants into silicon using various implantation energies (15, 35 and 70keV) and two silicon surface terminations; (i) a high quality (device) thermal oxide and (ii) native oxide. Characteristic spectral lines (and intensities) are used to identify dopants and radicals (e.g. $P_b$) which constitute electronic trap states.

Representative ESR spectra for the implanted samples are presented in Figure 5.5 where the resonance lines have been identified according to their g-factor. The dominant line in all of the spectra is the $P_b$ electron trap (dangling bond in $SiO_2$) at ~3365G. A hyperfine split P doublet (42G splitting centred at 3380G) is also evident. A central line due to exchange coupled P pairs or clusters (P-P) is also observed in some cases. Listed in Table 5.2 are the experimental P signal contributions (relative to that at 70 keV) compared with a simple theoretical prediction based on the donor concentrations.

The overwhelming feature of the ESR spectra are the $P_b$ signals. This is indicative of a high density of charge traps and although it might be expected for silicon terminated with a native oxide, it is also significant in this batch of thermal oxides. An over abundance of interface charge traps are not desirable if donors are to be placed near the surface using low energy implantation techniques. In the case of a native oxide, we find that the recovered ESR signal for donors placed further from the Si-$SiO_2$ interface (green circled data in Table 5.2) is higher than those closer to the interface (red circled data). This is especially true for the central line (exchange coupled or clustered donors). The loss of donor signal is also more pronounced in the native oxide (compared with the thermal oxide) terminated samples (i.e. red vs blue data) where there are a higher density of charge traps and surface defects [4, 5]. Overall there is a strong indication that the donors are ionised at low temperatures because they are placed nearer to the silicon surface (i.e. donors are effectively compensated by the traps). This represents a significant challenge for silicon QC engineering using the 'Top Down' approach where it is clear that best quality oxides will be required.

**Photoluminescence Spectroscopy and Donor Interactions in Ion Implanted Ensembles.** Further consideration of the work performed in collaboration with Prof. M. Thewalt (Canada) suggested that donor interactions may also studied using photoluminescence emission spectroscopy (PL). In silicon, above bandgap illumination produces electron-hole pairs which can bind to impurities on silicon lattice sites. The radiative recombination of these excitons produces near infrared emissions which can be used to spectroscopically identify impurities with very high sensitivity.

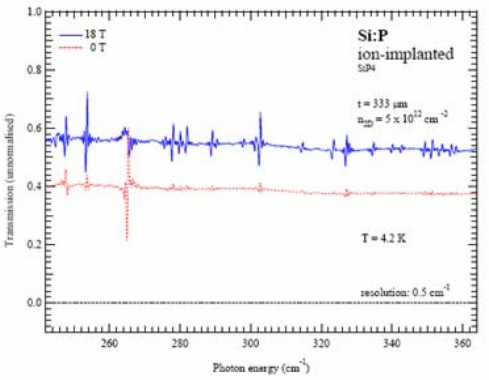


Figure 5.3. Spectrum of an ion-implanted dimer sample of Si(P) in both zero magnetic field (bottom, dashed, red line) and in magnetic field of 18T (top, full, blue line).

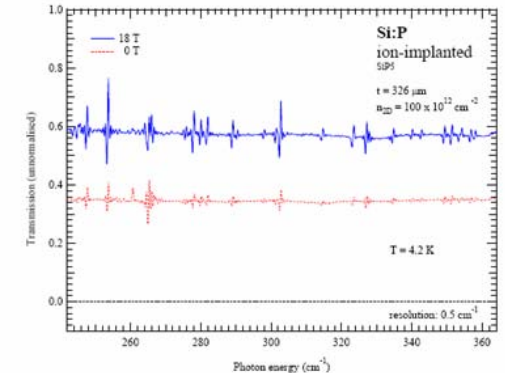


Figure 5.4. Spectrum of an ion-implanted sample of Si(P) in both zero magnetic field (bottom, dashed, red line) and in magnetic field of 18T (top, full, blue line).

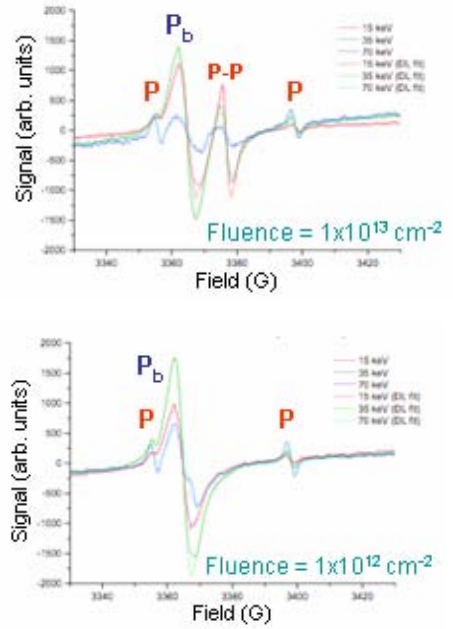


Figure 5.5. ESR spectra and fits for the samples with ~5 nm thermal oxide: a) implanted with $1x10^{13}$ $cm^{-2}$ fluence and energies of 15, 35 and 70 keV, b) implanted with $1x10^{12}$ $cm^{-2}$ fluence and the same energies.

| | | | Measured Contributions | | Calculated Contributions^ | | |
|---|---|---|---|---|---|---|---|
| Oxide | D ($cm^2$) | E (keV) | Doublet S% | Central S% | Doublet S% | Central S% | % Loss to |
| Native | $1x10^{13}$ | 15^ | 15.29 | 1.11 | 7 | 93 | |
| | | 40 # | 24.24 | 75.76 | 14 | 86 | |
| | | 70 | 24.66 | 75.33 | 33 | 67 | |
| Native | $1x10^{12}$ | 15^ | 35.32 | 2.21 | 57 | 43 | |
| | | 40^ | 51.88 | 0 | 69 | 31 | |
| | | 70 # | 100 | 0 | 100 | 0 | |
| Thermal | $1x10^{13}$ | 15^ | 6.92 | 71.35 | 5 | 93 | 2 |
| | | 35 | 11.62 | 88.37 | 14 | 86 | |
| | | 70 | 9.59 | 90.41 | 33 | 67 | |
| Thermal | $1x10^{12}$ | 15^ | 33.72 | 0 | 54 | 43 | 2 |
| | | 35^ | 44.36 | 0 | 69 | 31 | |
| | | 70 | 90 | 10 | 100 | 0 | |

Table 5.2. Comparison of experimental and theoretical allocations for the P donor signals.

^Normalised using the 70keV ESR

Traditionally, PL has been used extensively to monitor dopant activation, compensation and strain in bulk doped and epi-layer materials but may also be employed to study phosphorus doped ensemble in nano-layers produced using low energy ion implantation techniques.

Photoluminescence emission spectra for several ion implanted samples are presented in Figure 5.6 [6] where it is clear that there are two dominant spectral features. This first is the $P_{NP}$ transition arising from isolated (non-interacting) P donors. The second is the $P_{NP}$ cluster band which appears as a broad transition (coloured) and arises from excitons bound to clusters of interacting P donors. The centre of the cluster band appears to shift with increasing P concentration which was controlled using the implantation ion fluence and energy.

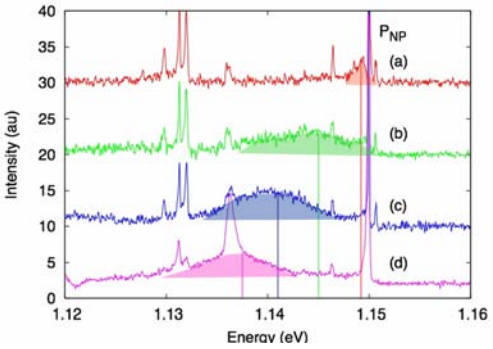


Figure 5.6. Low temperature Si:P photoluminescence from ion implanted ensembles. Samples were prepared as: (a) 70keV $P^+$; fluence: $1x10^{12}$ $cm^2$, (b) 70keV $P^+$; fluence: $5x10^{12}$ $cm^{-2}$, (c) 70keV $P^+$; fluence: $1x10^{13}$ $cm^{-2}$ and (d) 35keV $P^+$; fluence: $1x10^{13}$ $cm^{-2}$. Coloured lines indicate the approximate position of the centre of the $P_{NP}$ cluster band.

The shift in the cluster band energy can be modelled using various expressions including that proposed by Openov [7] who calculated the energy shift associated with forming a donor molecular state (hydrogenic) with wavefunctions that are symmetric and antisymmetric (split) between the donor pair. The model fit to the data using this expression is shown in Figure 5.7 (red triangles) which appears to model average donor pair separations down to ~5nm quite well. The shift in the cluster peak edge can also be modelled as a consequence of band gap narrowing [8] which has been observed with higher doping levels in silicon. In this context, the cluster peak may arise from a shrinking band gap in the implanted region accompanying the formation of a dopant band. The fit of the band edge shift to this model is also plotted in Figure 5.7 (green squares) with deviations evident at average donor separations below ~7nm.

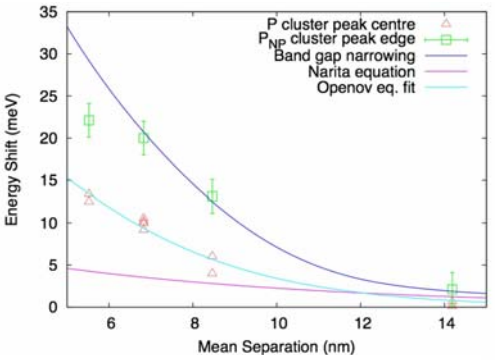


Figure 5.7. Fits to the experimental data using models for band energy and peak edge shifts of the P clusters.

**Electronic Raman Spectroscopy of Si:P in Bulk and Ion Implanted Ensembles.** Following on from the Raman work performed in 2006 using an in-house developed micro-Raman spectrometer, 2008 has seen the complete installation and commissioning a new, commercial, near-infrared, micro-Raman spectrometer. Located at the Bio21 Molecular Science and Biotechnology Institute at the University of Melbourne, this instrument was custom built by Renishaw plc (UK) and is well suited to electronic Raman and photoluminescence measurements of dopants in silicon. A photograph of the installed system is shown in Figure 5.8.

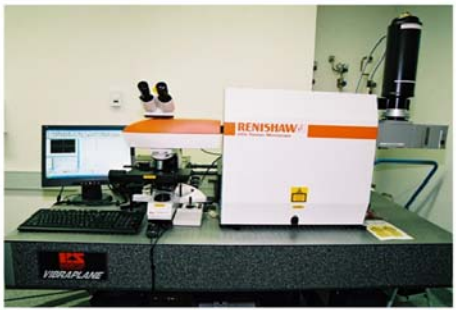


Figure 5.8. Photograph of the new Renishaw Reflex Invia micro-Raman spectrometer commissioned in 2008.

The instrument is equipped with dual laser excitation sources and multichannel detectors (both VIS and NIR) which allow rapid spectral acquisition which is crucial during low temperature measurement. This feature was considered particularly important since we use the phononic response of silicon to independently determine the sample temperature in the laser irradiated volume during measurement.

Electronic Raman measurements of the Si:P system provide an opportunity to study donor wavefunction overlap and ultimately measure interqubit coupling (i.e. exchange coupling) as proposed by Koiller et al [9]. A representative spectrum of bulk doped Si:P measured at 77K on the new instrument is shown in Figure 5.9. Here, transitions arising from the silicon band edge PL, phonons and impurities are all clearly evident even at these relatively high temperatures.

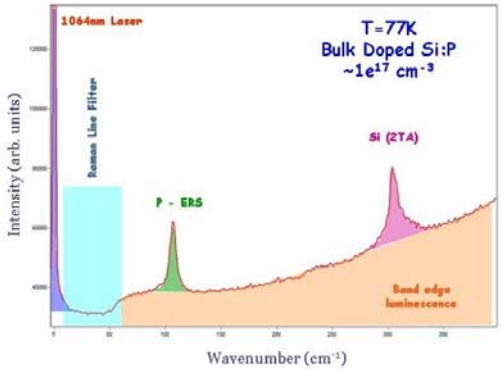


Figure 5.9. Spectroscopy of bulk doped Si:P ($\sim 1x10^{17}$ $cm^{-3}$) when using 1064nm (NIR) laser excitation. Spectral features have been *colourised* for identification and include: a Rayleigh scattered laser peak at $0cm^{-1}$, the spectral profile of the Raman Notch (line) filter, silicon band edge luminescence, a second order silicon acoustic phonon (2TA) and the phosphorus donor $1S(A_1)$ to $1S(E)$ electronic transition (i.e. absorption) at $\sim 106cm^{-1}$.

The temperature dependence of the phosphorus donor transition (P-ERS) was studied where thermal ionisation (>70K) should be the dominant reason for Raman signal reduction. The P donor transition intensity at $\sim 106cm^{-1}$ was plotted as a function of temperature and compared with the theoretical donor ground state occupation probabilities (i.e. Fermi-Dirac statistics). This comparison is shown in Figure 5.10 where it is clear that the exponential behaviour of the signal intensity is mirrored by the occupation statistics.

Low temperature (< 40K) measurements were also performed on bulk doped Si:P samples. In addition to controlling the substrate temperature, the donor concentration and direction of polarisation of the electric vector (incident and scattered) were controlled with the results shown in Figure 5.11. A number of overlapping transitions are evident which evolve both with temperature and polarisation. The reason for the polarisation dependence is not understood given the bulk (random) nature of the doping so further investigation is underway. In addition, many of these transitions are unidentified and thus require further studies with modelling. Although ion implanted ensembles were also investigated in a similar manner, no donor transitions were observed. This may be due to the smaller number of donors in the measurement volume compared with the bulk doped substrates leading to reduced signal intensities.

While the $1S(A_1) - 1S(E)$ donor transition has not yet been observed in implanted Si:P ensembles, single particle continuum scattering has. This signal arises from electrons being scattered out of the conduction band (CB) giving rise to CB charge density fluctuations (see the diagram inset in Figure 5.12). This signal is often observed with highly doped (metallic) samples. Some examples of single particle spectra are shown in Figure 5.12. It is interesting to note that the metallic substrate (<0.01 Ω.cm) and the 15keV P+ implanted ensemble have similar (exponential) features whereas the 10keV $P_2^+$ (molecular) implant has a different spectral profile. The 10keV $P_2^+$ implant was also investigated using ESR with the resulting spectrum shown as an inset in Figure 5.12. The ESR spectrum has a free electron peak characteristic of highly (metallic) doping even though the peak P concentration is <Mott transition. These results suggest that these techniques can also be used to study donor-donor interactions (i.e. clustering) with very high sensitivity even in the implanted substrates.

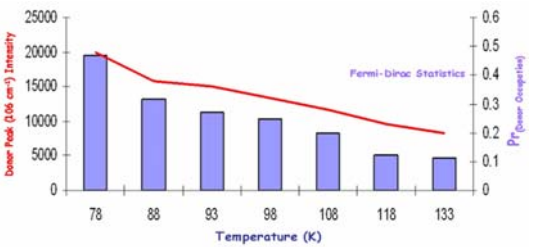


Figure 5.10. Temperature dependence of the donor transition intensity at ~106cm$^{-1}$ (red line). For comparison, the probability of finding an unionised (thermally) donor is also plotted (columns).

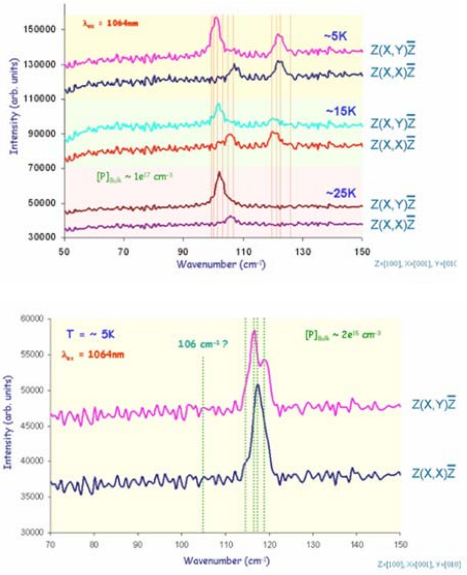


Figure 5.11. Polarised NIR micro-Raman measurements of bulk doped Si:P at low temperatures.

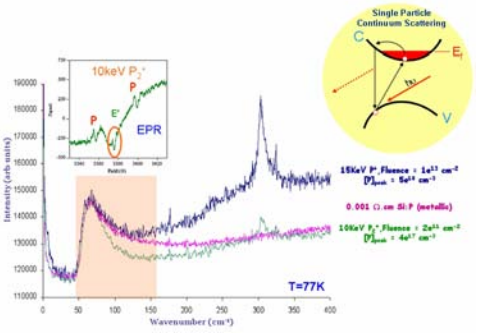


Figure 5.12. Single particle scattering from bulk doped (metallic) and ion implanted Si:P. The inset ESR spectrum is also from the 10keV molecular P implant.

## Bibliography


[1] R.A. Lewis *et al*., Proceedings of the 18th Biennial Australian Institute of Physics Congress Adelaide, 30th Nov. to 5th Dec. 2008, Australia (submitted).

[2] P.G. Spizzirri *et al*., Proceedings of the 15th biennial Nuclear and Complementary Techniques of Analysis Conference (NCTA), University of Melbourne, 21st – 23rd Nov. 2007, Australia.

[3] N. Bulatovic *et al*.; Proceedings of 32nd Condensed Matter and Materials Meeting, 30th Jan. – 1st Feb. 2008, Australia.

[4] P.G. Spizzirri *et al*., Proceedings of the 15th biennial Nuclear and Complementary Techniques of Analysis Conference (NCTA), University of Melbourne, 21 - 23 Nov. 2007, Australia.

[5] P.G. Spizzirri *et al*., Proceedings of the 15th biennial Nuclear and Complementary Techniques of Analysis Conference (NCTA), University of Melbourne, 21 - 23 Nov. 2007, Australia.

[6] N. Stavrias, International Conference on Nanoscience and Nanotechnology, Melbourne, 25-29 Feb. 2008, Australia.

[7] L. Openov, Phys. Rev. B 70, 233313 (2004).

[8] D.B.M. Klaassen *et al*, Sol. Stat. Elect. 35, 125 (1992)

[9] B. Koiller, Phys. Rev. Lett. 90, 067401 (2003).

[10] P.G. Spizzirri *et al*., International Union of Materials and Research Societies (IUMRS) and the International Conference on electronic materials, 28th July to 1st Aug. 2008, Sydney Australia.

## D6. MATERIALS RESEARCH

Over the 2004–2008 reporting period the Materials program has been faced with the challenge of finding optimum processing conditions and appropriate methods of analysis for an increasing range of fabrication parameters and device structures. We began in 2004 with the problem of how to activate low densities of phosphorus implanted at energies less than 20 keV with a minimal thermal budget that resulted in minimal phosphorus diffusion and yet was sufficient to achieve extremely low levels of charge traps. In 2008 we are dealing with a greater variety of device structures including gate-defined silicon quantum dot structures implanted at low fluences with keV phosphorus ions and spin-dependent transport devices requiring high fluence As implanted source-drain leads. Along the way we have acquired a greatly expanded suite of analytical techniques and expertise to provide the necessary diagnostics of the structures formed. Some of the key techniques include capacitance-voltage and deep level transient spectroscopy analysis of electrical characteristics and charge trap densities, ellipsometric measurement and mapping of oxide thickness and focussed-ion beam sectioning and transmission electron microscopy imaging of device structures with high precision selection of regions of interest.

In the 2004–2005 reporting period key achievements included:

- Measurement of interface charge trap densities in as-grown and H-passivated MOS structures.
- Demonstration that annealing strategy leads to high level of dopant activation for intermediate dose equivalent to 60 donors per cluster.
- Kelvin force microscopy measurements of as-implanted and annealed oxides showing oxide repair.

Figure 6.1 shows results from the dopant-activation study. The four-point probe measurement of dopant activation for P, 15 keV, $1 \times 10^{13}$ $cm^{-2}$ implants into high-resistivity B-doped substrates capped with a 5nm thermally grown oxide showed that for anneals in the 1000−1050°C range greater than 80% activation could be achieved for a 5 s rapid thermal anneal.

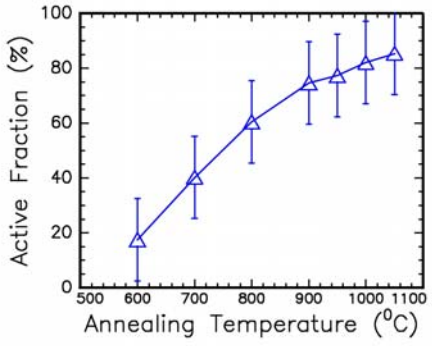


Figure 6.1: Activation fraction of P donors versus annealing temperature for 5s anneals of P, 15 keV, $1 \times 10^{13}$ $cm^{-2}$ implants into high-resistivity B-doped substrates capped with a 5nm thermally-grown oxide. 5nm thermally grown oxide.

In the 2005–2006 reporting period key achievements included:

- First DLTS measurements of interface trap densities for a 5 nm oxide implanted with 15 keV P to a fluence of $1\times 10^{11}$P/$cm^2$ and then rapid thermally annealed at 1100°C, 5s prior to capacitor formation showing that good oxide recovery was achieved and the implanted oxide exhibited only a small increase in interface trap density compared to that of an un-implanted oxide (Figure 6.2).
- Commencement of transmission electron microscopy studies of gate oxide and interfaces characteristics.

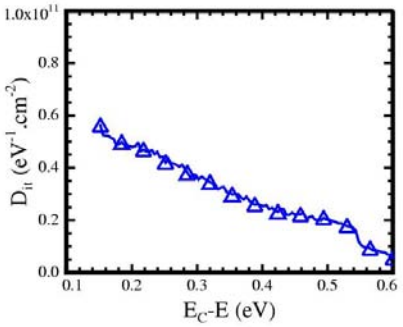


Figure 6.2: DLTS measurements of interface trap densities for a 5 nm oxide implanted with 15 keV P to a fluence of $1\times 10^{11}$P/$cm^2$ and then rapid thermally annealed at 1100°C, 5s prior to capacitor formation.

In the 2006–2007 reporting period key achievements included:

- Observation of a marked improvement in interface trap density for ion implanted and rapid thermally annealed oxides when the starting trap density in the as-grown oxides was relatively high (Figure 6.3).
- Development of spectroscopic ellipsometry capability for accurate measurement and spatial mapping of the gate oxide thickness on device wafers.
- Development of focussed ion beam capability for cross-sectioning of quantum computer device structures so that transmission electron microscopy can be used to examine all of the layers, interfaces and interconnects in selected regions of fully fabricated devices.

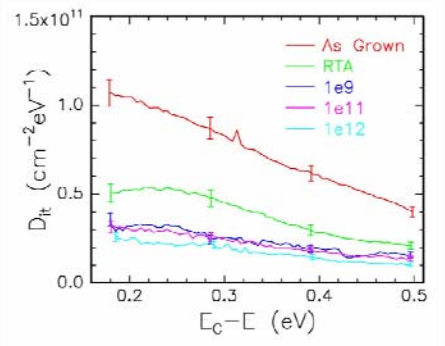


Figure 6.3. Interface trap density, $D_{it}$, versus trap energy relative to the conduction band edge obtained from DLTS measurements for nominally 5nm thick thermal oxides implanted with 15 keV P to various fluences, followed by RTA annealing and H-passivation.

The current reporting period began on a low with unacceptably high interface trap densities in our high-quality thermal oxides and it ended on a high with the lowest trap densities that we have ever recorded. In between, there was a lot of meticulous detective work required to isolate the source of the contamination leading to the high trap densities and some interesting new effects of ion implantation on trap densities for through oxide implants have been observed. By the end of 2007 the information gained from this painstaking work has put the Centre in a much stronger position in terms of its ability to produce high quality materials suitable for quantum device fabrication.

Key achievements in the 2007-2008 reporting period include:

- Achievement of an interface trap density towards the band edge of $<1\times10^{10}eV^{-1}.cm^{-2}$ This is the lowest trap density that we have achieved thus far and is expected to be suitable for successful fabrication of quantum devices.
- First measurement of fixed oxide charge density in our field oxides. Outcomes from this work are feeding into development of a guard ring structure to prevent source-drain leakage from occurring in our devices.
- Development of a better understanding of the effects of various processing steps including rapid thermal annealing effects on interface state densities in the low density regime and the role of the post-metallisation Al-anneal on defect densities.
- FIB cross-sectioning and TEM analysis of double quantum dot structures.

**Achieving Interface trap density < $10^{10}$eV$^{-1}$.cm$^{-2}$.** Figure 6.4 shows interface trap density versus position in the band-gap with respect to the conduction band edge for a 5nm thermal oxide that has been prepared under optimal conditions. The data show that we can achieve a trap density < $10^{10}$eV$^{-1}$.cm$^{-2}$ towards the conduction band edge and gives us great encouragement that our quantum devices can be produced with suitably low trap densities.

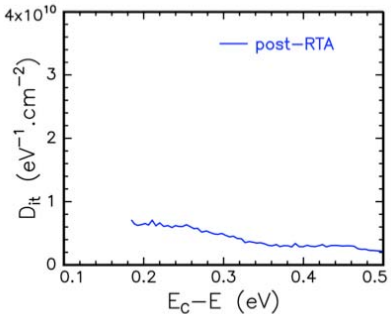


Figure 6.4: Interface trap density versus position in the band-gap referenced to the conduction band edge for a 5nm thermal oxide that has been prepared under optimal conditions.

**Fixed Oxide Charge.** Preliminary capacitance-voltage (C-V) measurements have been performed on metal-oxide semiconductor (MOS) capacitors in order to determine the fixed oxide charge in thick field oxides grown by the CQCT. The effect of a post-oxidation forming gas anneal on the fixed oxide charge has also been determined. Figure 6.5 shows the C-V measurements from an annealed sample. Different oxide thicknesses were produced by etching the as-grown wafer (sample B1 in Figure 6.5) for various times. The flat band voltage of these curves as a function of the oxide thickness can be related to the fixed oxide charge density as shown in Figure 6.5. This method yield fixed oxide charge densities of (2.1±0.1) × $10^{11}$ cm$^{-2}$ and (1.85±0.07) × $10^{11}$ cm$^{-2}$ for the un-annealed and anneal samples respectively.

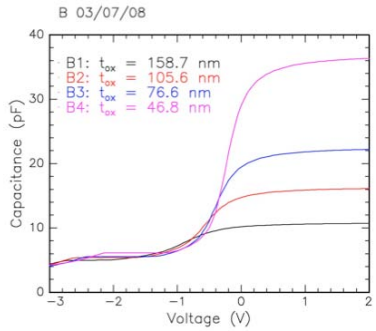


Figure 6.5: Capacitance-Voltage curves for the field oxide having undergone a post-oxidation anneal and various etches to thicknesses indicated in the figure.

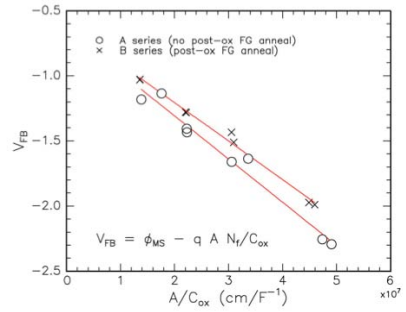


Figure 6.6: Flat band voltage determined from the C-V curves as a function of the A/$C_{ox}$ for the etched back field oxides.

**Effect of Post-Metallization Al-Anneal.** Deep level transient spectroscopy (DLTS) has been used to characterize the defects in MOS capacitors with 5 nm high-quality oxides after different processing schedules. It has recently been found that a post-metallization anneal is essential to reduce the silicon/oxide interface trap densities to an acceptable level. Figure 6.7 shows the raw DLTS data from a 5 nm oxide which did not have a post-metallization anneal. A large asymmetric peak was found which indicates a large concentration of defects. The peak shows some unusual characteristics and is not indicative of a standard bulk or silicon-oxide interface type defect. This has hindered its identification. Furthermore, standard DLTS and C-V analysis cannot be performed on such a sample.

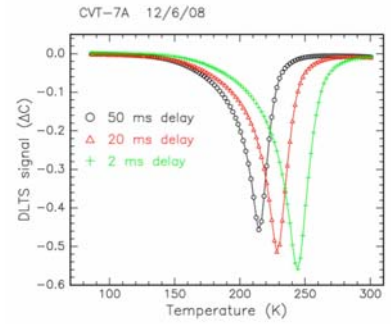


Figure 6.7: The raw DLTS signal versus temperature for nominally 5 nm thick thermal oxides without a post-metallization anneal.

Figure 6.8 shows the C-V profiles of the sample in Figure 6.6 (dashed line) as well as samples after various annealing schedules. As the annealing temperature approaches 400C the C-V curves approach the ideal form as indicated by the arrow in the figure.

The peak shown in Figure 6.7 also disappears after an anneal of 300°C for 15 minutes. However, the interface defect densities are still quite high (not shown). Figure 6.9 shows the interface trap densities for 5 nm oxides after an anneal at 400°C for 15 minutes. Such an anneal schedule is sufficient to remove the peak shown in Figure 6 and reduce the $D_{it}$ value to an acceptable level.

**Focussed-ion beam cross-sectioning of device structures.** FIB cross-sectioning of quantum device structures continues to be an extremely important diagnostic tool for the Centre. This series of images shows details of a double-island gate defined silicon quantum dot structure that is currently being studied in the quantum measurement program. Figure 6.10 is an expanded view of the device while Figure 6.11 shows a close-up of one of the double quantum dot structures revealing details of the finger structures used to define the double quantum dots and the overlying top gate. Figure 6.12 is a bright-field transmission electron micrograph of a cross-section through the three aluminium gate fingers showing details of the aluminium oxide interfacial regions surrounding each finger. These provide electrical isolation between the various levels of metallisation and they are thicker and not as uniform as was expected. The relevant processing steps are being examined to see if the outcome can be improved for later generations of devices. In addition, knowledge of the actual oxide thickness and uniformity are being fed into the device measurement program.

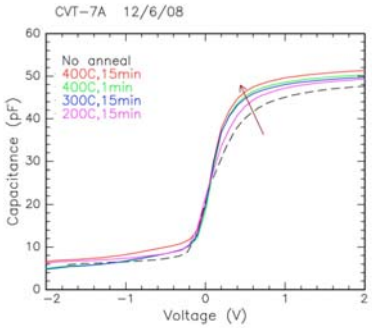


Figure 6.8: C-V curves for nominally 5 nm thick thermal oxides with the post-metallization anneal schedule as parameter showing that the C-V profile approaches ideality as the annealing temperature approaches 400°C.

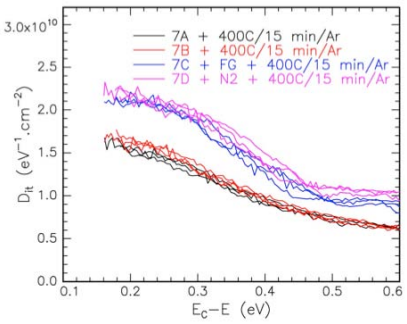


Figure 6.9: Interface trap densities, $D_{it}$, versus tap energy relative to the conduction band edge obtained from DLTS measurements on 5 nm oxides after various post-metallization anneals

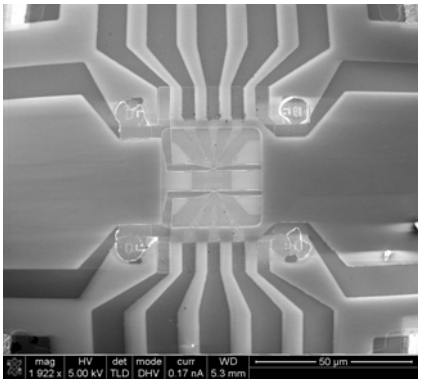

Figure 6.10: Scanning electron micrograph of double quantum dot gate defined silicon quantum dot structure.

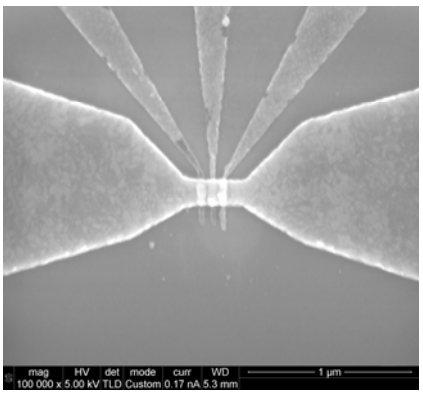

Figure 6.11: A close-up of one of the double quantum dot structures revealing details of the finger structures used to define the double quantum dots and the overlying top gate

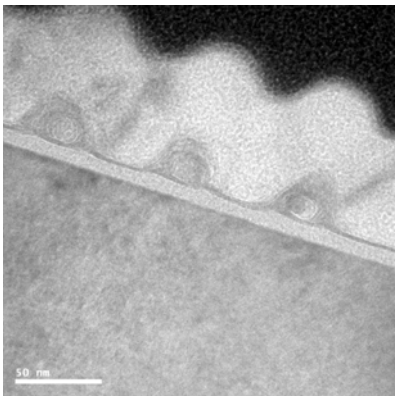

Figure 6.12: Transmission electron microscopy image of a cross-section through the three aluminium gate fingers showing details of the aluminium oxide interfacial regions surrounding each finger which provide electrical isolation between the various levels of metallisation.

**Bibliography**


[1] B.C. Johnson & J.C. McCallum, Physical Review B. 76, 045216 (2007).

[2] B.J. Villis & J.C. McCallum, Nuclear Instruments & Methods in Physics Research Section B - Beam Interact with Materials and Atoms 257, 212 (2007).

[3] B.C. Johnson *et al*., Physical Review B. 77: 2141091 (2008).